

Philipp Kögl, BSc

# **Application of a Spinning Disc Reactor for Amide Bond Formation in Water Using a Biomass-Based Polymeric Additive**

## **MASTER'S THESIS**

To achieve the university degree of

Master of Science

Master's degree program:

CHEMIE

submitted to

**Graz University of Technology**

## **Supervisors**

Kappe, Christian Oliver, Univ.-Prof. Mag. Dr.rer.nat.

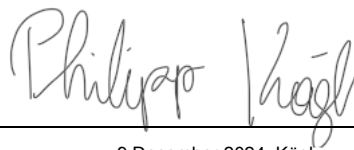
Institute of Chemistry

Ötvös, Sandor Balazs, Dr.

Institute of Chemistry

## AFFIDAVIT

I declare that I have authored this thesis independently, that I have not used other than the declared sources / resources, and that I have explicitly marked all material which has been quoted either literally or by content from the used sources. The text document uploaded to TUGRAZonline is identical to the present master's thesis.



---

9 December 2024, Kögl

## Acknowledgements

I would like to express my deepest gratitude to Prof. C. Oliver Kappe, for allowing me to conduct my master thesis in the CC Flow group and to gain valuable insight into the field, and of course my supervisor Dr. Sándor B. Ötvös for the guidance and continuous support throughout the course of my master thesis in flow chemistry. Their expertise and encouragement have been instrumental in shaping this research.

I am also thankful for my project partner Sabrina Kogler and the whole group at CC Flow for their support and shared expertise that was essential for the completion of this thesis.

Furthermore, I extend my appreciation to the resources and facilities provided by the University of Graz, the CC Flow group, and the RCPE, which have played a crucial role in conducting the experiments and analysis presented in this thesis. Additionally, I want to extend my gratitude towards the Physical & Theoretical Chemistry department for the expertise and the equipment they provided for the viscosity measurements.

Lastly, I am grateful to my friends, family and especially my girlfriend for their patience, encouragement, and continued support throughout my academic journey. Without them, I would have never come this far.

This thesis is a testament to the collaborative efforts of many, and I am sincerely thankful to everyone who has been part of this experience.

## Abstract

Modern synthetic organic chemistry depends heavily on organic solvents to dissolve substrates and accelerate reactions, but these solvents pose significant health and safety risks, including toxicity, flammability, and environmental impact. Contributing over 80 % of synthetic chemistry waste, they also drive issues like air pollution and climate change. Water based systems are a sustainable alternative, but poor solubility of reactants often slows reactions. Surface active additives like hydroxypropyl methylcellulose (HPMC), a biodegradable and non-toxic cellulose derivative, show promise in enabling aqueous organic synthesis. Efforts to improve amidation reactions, essential to the pharmaceutical industry, focus on safer coupling reagents like COMU. Specialized flow chemistry instrumentation is capable of providing efficient solutions for handling multiphasic mixtures, enhancing process control, safety, and operational flexibility.

A continuous flow process was developed and optimized for the amidation of 4-hydroxyphenyl acetic acid with 3,5-dimethylaniline to produce *N*-(3,5-dimethylphenyl)-2-(4-hydroxyphenyl)acetamide. The reaction utilized 2,6-lutidine as a base and COMU as the coupling reagent in a solvent system of 2 wt% HPMC/H<sub>2</sub>O. A comparative analysis of physical properties among HPMC variants identified Mantrocel® E5 as the optimal component for facilitating amide bond formation under flow conditions. In initial batch experiments we investigated the influence of stirring rate and temperature on the resulting slurry mixtures and the reaction performance. Key flow process parameters, including spinning speed of the reactor rotors, temperature, residence time, and reactant concentrations, were systematically optimized to maximize efficiency and product yield (77 % isolated yield). Additionally, quantitative green chemistry metrics were evaluated, highlighting the sustainability and environmental advantages of the optimized flow process. This study demonstrates the potential of employing HPMC based solvent systems and continuous flow technology for efficient and sustainable amidation reactions.

## Zusammenfassung

Die moderne synthetische organische Chemie ist in hohem Maße auf organische Lösungsmittel angewiesen, um Substrate zu lösen und Reaktionen zu beschleunigen. Diese Lösungsmittel bergen jedoch erhebliche Gesundheits- und Sicherheitsrisiken, darunter Toxizität, Entflammbarkeit und Umweltbelastung. Sie machen mehr als 80 % des Abfalls in der synthetischen Chemie aus und sind auch für Probleme wie Luftverschmutzung und Klimawandel verantwortlich. Systeme auf Wasserbasis sind eine nachhaltige Alternative, aber die schlechte Löslichkeit der Reaktanten verlangsamt oft die Reaktionen. Oberflächenaktive Additive wie Hydroxypropylmethylcellulose (HPMC), ein biologisch abbaubares und ungiftiges Cellulosederivat, sind vielversprechend, um die wässrige organische Synthese zu ermöglichen. Die Bemühungen zur Verbesserung von Amidierungsreaktionen, die für die pharmazeutische Industrie wichtig sind, konzentrieren sich auf sicherere Kopplungsreagenzien wie COMU. Spezielle Instrumente für die Fließchemie bieten effiziente Lösungen für die Handhabung mehrphasiger Gemische und verbessern die Prozesskontrolle, die Sicherheit und die betriebliche Flexibilität.

Es wurde ein kontinuierliches Fließverfahren für die Amidierung von 4-Hydroxyphenyl-essigsäure mit 3,5-Dimethylanilin zur Herstellung von *N*-(3,5-Dimethylphenyl)-2-(4-hydroxyphenyl)acetamid entwickelt und optimiert. Bei der Reaktion wurde 2,6-Lutidin als Base und COMU als Kupplungsreagenz in einem Lösungsmittelsystem aus 2 Gew.-% HPMC/H<sub>2</sub>O verwendet. Eine vergleichende Analyse der physikalischen Eigenschaften der verschiedenen HPMC-Varianten ergab, dass Mantrocel® E5 die optimale Komponente ist, um die Bildung von Amidbindungen unter Fließbedingungen zu erleichtern. In ersten Batch-Experimenten untersuchten wir den Einfluss von Rührgeschwindigkeit und Temperatur auf die resultierenden Aufschlämmungsmischungen und die Reaktionsleistung. Die wichtigsten Parameter des Fließprozesses, einschließlich der Drehgeschwindigkeit der Reaktorrotoren, der Temperatur, der Verweilzeit und der Reaktantenkonzentrationen, wurden systematisch optimiert, um die Effizienz und die Produktausbeute (77 % isolierte Ausbeute) zu maximieren. Darüber hinaus wurden die quantitativen Kennzahlen der grünen Chemie ausgewertet, um die Nachhaltigkeit und die Umweltvorteile des optimierten Fließprozesses hervorzuheben. Diese Studie zeigt das Potenzial des Einsatzes von HPMC-basierten Lösungsmittelsystemen und kontinuierlicher Durchflusstechnik für effiziente und nachhaltige Amidierungsreaktionen.

## List of abbreviations

<b>1</b>	4-hydroxyphenyl acetic acid
<b>2</b>	3,5-dimethylaniline = 3,5-xylidine
<b>3</b>	2,6-lutidine
<b>4</b>	COMU = (1-cyano-2-ethoxy-2-oxoethylidenaminoxy)dimethylamino-morpholino-carbenium-hexafluorophosphate
<b>5</b>	<i>N</i> -(3,5-dimethylphenyl)-2-(4-hydroxyphenyl)acetamide
<b>6</b>	<i>N,N</i> -dimethylmorpholine-4-carboxamide
<b>7</b>	ethyl 2-cyano-2-nitrosoacetate
BPR	back-pressure regulator
CDCl <sub>3</sub>	deuterated chloroform
CH <sub>3</sub> CN	acetonitrile
DCC	<i>N,N'</i> -dicyclohexyl-carbodiimide
DCM	dichloromethane
DMSO-d <sub>6</sub>	deuterated dimethyl sulfoxide
EDC	<i>N</i> -(3-dimethylaminopropyl)- <i>N'</i> -ethylcarbodiimide
<b>Efaproxiral</b>	2-(4-{2-[(3,5-dimethylphenyl)amino]-2-oxoethyl}phenoxy)-2-methylpropanoic acid
eq	equivalent(s)
EtOAc	ethyl acetate
GC-MS	gas chromatography – mass spectrometer
HPLC	high pressure liquid chromatography
HPMC	hydroxypropyl methylcellulose
iPrOAc	isopropyl acetate
iPrOH	isopropanol
M	mol*L <sup>-1</sup>
NMR	nuclear magnetic resonance
PEEK	Polyether ether ketone
PFA	Perfluoro alkoxy alkanes
RTD	residence time distribution
TFA	trifluoroacetic acid
TLC	thin layer chromatography
UV	ultraviolet (light)
VIS	visible (light)
wt%	weight percentage(s)

## List of figures

Figure 1: <b>A</b> - Chemical structure of HPMC; <b>B</b> - Possible folding of HPMC in water.....	10
Figure 2: Structures of DCC, EDC, Oxyma and COMU .....	12
Figure 3: Simplified representation of a single disc of the SpinPro R10. ....	14
Figure 4: Illustration of the reactor setup used in the RTD studies. ....	16
Figure 5: Schematic representation of the continuous flow setup for the synthesis of product <b>1</b> with COMU in the SpinPro R10 reactor. ....	18
Figure 6: Setup for the synthesis of <b>1</b> with COMU in the SpinPro R10 reactor.....	19
Figure 7: Average viscosity measurement of 2 wt% HPMC/H <sub>2</sub> O solutions at 25 °C.....	21
Figure 8: Demonstration of the washing step with DCM. ....	25
Figure 9: RTD of distilled water at various flow rates and a fixed spinning speed of 2000 rpm at 25 °C in the SpinPro R10. ....	26
Figure 10: RTD-studies with distilled water in the SpinPro R10 at 25 °C and fixed flow rates with different spinning speeds. ....	27
Figure 11: RTD studies for different media in the SpinPro R10 at 2000 rpm.....	28
Figure 12: Stability tests for the synthesis of product <b>5</b> in the SpinPro R10. ....	30
Figure 13: Viscosity measurement of 2 wt% HPMC/H <sub>2</sub> O solutions at 40 °C.....	38
Figure 14: Viscosity measurement of 2 wt% HPMC/H <sub>2</sub> O solutions at 60 °C.....	38
Figure 15: RTD studies for different media in the SpinPro R10 at 1001 rpm.....	40
Figure 16: RTD studies for different media in the SpinPro R10 at 4000 rpm.....	41
Figure 17: Stability tests for the synthesis of product <b>5</b> in the SpinPro R10. ....	41
Figure 18: Calibration of product <b>5</b> measured with HPLC-UV/VIS at 215 nm.....	42
Figure 19: <sup>1</sup> H-NMR of the pure product, isolated from a flow run. ....	43
Figure 20: <sup>13</sup> C-NMR of the pure product, isolated from a flow run.....	43

## List of tables

Table 1: Results of viscosity measurements of the aqueous HPMC solutions at different temperatures. ....	20
Table 2: Effects of the stirring rate with different HPMC variants in 1 mL scale batch reactions. ....	23
Table 3: Effects of increasing temperature with different HPMC variants in 1 mL scale batch reactions.....	24
Table 4: Results for the isolated yields of product <b>5</b> with different solvents used in the last step of the work-up.....	25
Table 5: Used parameters for RTD studies.....	26
Table 6: RTD results for different residence times using distilled water at 25 °C and 2000 rpm in the SpinPro R10. ....	27
Table 7: Results for the reproducibility tests of the model reaction performed at different spinning speeds in the SpinPro R10.....	29
Table 8: Temperature and residence time optimization performed in the SpinPro R10.....	30
Table 9: Results for the concentration optimizations performed in the SpinPro R10. ....	31
Table 10: Calculated quantitative green metrics for the synthesis of product <b>5</b> in the optimized flow process utilizing COMU.....	32
Table 11: Results for solubility tests to remove decomposition product <b>A</b> of COMU. ....	39
Table 12: RTD statistic in the SpinPro R10 for distilled water with various flow rates and rotation speeds at 25 °C.....	39
Table 13: RTD statistic in the SpinPro R10 for 2 wt% HPMC E5 at various flow rates and rotation speeds.....	40
Table 14: Values used for the assessment of green metrics for the synthesis of product <b>5</b> in flow with COMU.....	42



## TABLE OF CONTENTS

AFFIDAVIT .....	1
Acknowledgements .....	2
Abstract.....	3
Zusammenfassung .....	4
List of abbreviations.....	5
List of figures .....	6
List of tables.....	7
1. Introduction .....	9
1.1. Green Chemistry.....	9
1.2. Chemistry in water .....	10
1.3. Amide bond formation .....	11
1.4. Continuous flow chemistry.....	13
2. Experimental.....	15
2.1. Materials and general information .....	15
2.2. Preparation of HPMC solutions .....	16
2.3. Residence time distribution study.....	16
2.4. General batch procedure using COMU as coupling reagent .....	17
2.5. Continuous flow reactor setup.....	18
2.6. General procedure for reactions in flow .....	19
3. Results and Discussion .....	20
3.1. Characterization of aqueous HPMC mixtures .....	20
3.2. Preliminary batch experiments .....	21
3.3. Work-up strategies for the synthesis of <b>1</b> with COMU.....	25
3.4. Residence time distribution .....	26
3.5. Flow process optimization .....	29
3.6. Green metrics .....	32
3.7. Conclusion and Outlook .....	33
4. References .....	34
5. Appendix.....	38

## 1. Introduction

### 1.1. Green Chemistry

Green chemistry, related to sustainable chemistry and circular chemistry, is a field within chemistry and chemical engineering dedicated to designing products and processes that reduce or eliminate the utilization and production of hazardous substances.<sup>1</sup> Unlike environmental chemistry, which studies the effects of pollutants on the natural environment, green chemistry focuses on minimizing the environmental impact of chemical practices by reducing the consumption of non-renewable resources, efficiently utilizing raw materials, ideally renewable ones, eliminating waste, and avoiding the use of toxic or hazardous reagents and solvents in the production and application of chemical products.<sup>2-8</sup> In 1998, twelve principles were published to guide the practice of green chemistry, providing various strategies for the reduction of environmental and health impacts of chemical production and present research priorities for the development of green chemistry technologies.<sup>9</sup>

Modern synthetic organic chemistry, both in research and industry, heavily depends on the utilization of organic solvents, which are required to dissolve substrates and facilitate faster reactions by bringing reactants into close proximity.<sup>10-16</sup> As a result, most reactions use anhydrous organic solvents to exclude water, which is often perceived as an impediment to chemical reactivity, despite their severe toxicological and environmental risks. Organic solvents are frequently toxic, with properties such as carcinogenicity, mutagenicity, teratogenicity and reproductive toxicity (CMR) posing serious health risks. Additionally, their flammability, explosiveness, and potential for accidental exposure amplify the dangers, particularly in industrial settings. From an environmental perspective, these solvents contribute significantly to air pollution, ground level ozone production, and climate change.<sup>11,14</sup> The reliance on organic solvents is responsible for over 80 % of the waste generated in synthetic chemistry, with many solvents not being recycled, further exacerbating the problem. While the utilization of organic solvents was once a breakthrough enabling efficient chemical reactions, the long-term consequences have sparked a global movement toward greener alternatives.<sup>10-12,14,17-23</sup> Regulations like the European Registration, Evaluation, Authorization, and Restriction of Chemicals (REACH) regulation, implemented in 2006, aim to mitigate these risks by encouraging the development of environmentally friendly methods.<sup>14</sup> While solvent-free reactions present an ideal solution, their applicability is limited. Consequently, researchers are exploring greener alternatives, drawing inspiration from nature, where reactions occur in aqueous environments without the need for organic solvents, even when substrates are not water-soluble.<sup>12,14</sup> Nevertheless, transitioning to water-based systems is challenging, as many traditional reaction components exhibit poor solubility in water, leading to reduced reaction rates or failure. Overcoming these limitations is critical for developing more sustainable and environmentally friendly synthetic processes.

## 1.2. Chemistry in water

To address the challenges of limited solubility and slow reaction rates in water, the concept of surface active additives has emerged as a promising solution for enabling organic synthesis in aqueous environments. This approach leverages micellar conditions, where surfactants self-assemble into micelles that act as nanoreactors, effectively creating a lipophilic core within an aqueous medium.<sup>24-29</sup> These micelles mimic the behavior of organic solvents, providing a concentrated reaction environment that enhances reaction rates and yields. As a result, micellar chemistry opens new avenues for sustainable and environmentally friendly synthetic processes. The success of reactions under micellar conditions depends heavily on the properties of the amphiphilic surfactants utilized. In response, a variety of designer surfactants, such as TPGS-750-M or PS-750-M, have been specifically engineered to facilitate diverse transformations in water.<sup>30-32</sup> While these surfactants offer significant benefits, including broader reaction applicability and reduced environmental impact, their use is not without drawbacks. The production of designer surfactants can be very expensive, and some of them can be regarded as toxic. Additionally, their effective application as enablers in aqueous reaction mixtures often necessitate the utilization of co-solvents to achieve uniform mixing and optimal yields.<sup>10,26,33</sup> As a result, a broad selection of commercially available surfactants has been developed, including more economical alternatives.<sup>33</sup>

Hydroxypropyl methylcellulose (HPMC), commonly known as Hypromellose, has recently gained attention as a promising surface active additive for facilitating chemical reactions in aqueous environments.<sup>34-36</sup> HPMC is a biodegradable, non-toxic, semisynthetic derivative of cellulose, produced through the alkaline hydrolysis of wood pulp followed by reaction with methyl chloride and propylene oxide. This process yields a hydrophilic and environmentally benign cellulose ether (figure 1A), widely applied in pharmaceuticals and the food industry as a drug delivery system and food additive.<sup>35-39</sup>

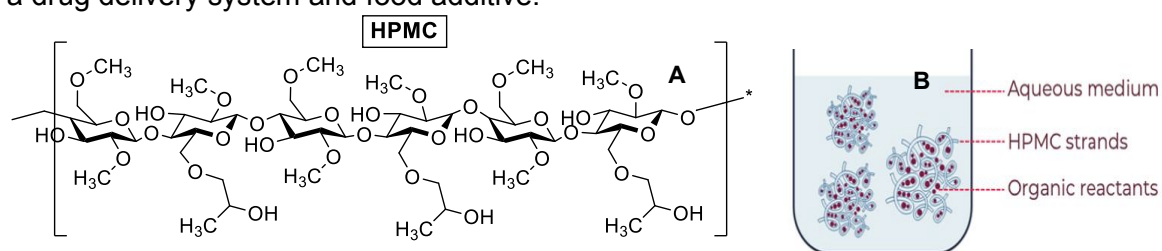


Figure 1: **A** - Chemical structure of HPMC; **B** - Possible folding of HPMC in water.<sup>10</sup>

The physicochemical properties of HPMC can be finely tuned by adjusting the substitution patterns of methoxy and hydroxypropyl groups, which significantly affect its viscosity, water solubility, and, in pharmaceutical applications, drug release profiles.<sup>39,40</sup> Commercially, HPMC is categorized into three main categories, (K, F, and E) based on substitution levels. For instance, grade K typically contains 19-24 % methoxy and 7-12 % hydroxypropyl groups, while grade E has higher methoxy levels of 28-30 % with similar hydroxypropyl content.<sup>37,39</sup>

In addition to its established applications as an excipient and drug delivery system in the pharmaceutical industry and as a food additive, HPMC has gained attention for its ability to self-aggregate and function as a surface active additive, enabling chemical reactions in aqueous media.<sup>35,38</sup>

Unlike conventional micelle-mediated chemistries, HPMC eliminates the need for co-solvents, aligning with green chemistry principles and offering a more sustainable approach.<sup>34,36,38</sup> When an aqueous solution of HPMC is heated, dehydration occurs within the polymer's interior, leading to a reduction in viscosity and the formation of hydrophobic pockets through the polymer coiling. These hydrophobic pockets serve as nanoreactors, facilitating organic reactions directly in water (figure 1B). However, the temperature range for this functionality is relatively narrow, as surpassing the thermal gelation threshold (approximately 60-65 °C, depending on the HPMC grade) typically results in the formation of viscous slurries or biphasic mixtures, significantly impeding mass transfer and limiting reaction conditions.<sup>35,37,41</sup> Despite these limitations, HPMC has been successfully utilized in a variety of aqueous phase reactions, including amide coupling, demonstrating its potential as a cost-effective, sustainable, and versatile alternative in modern synthetic chemistry.<sup>29</sup>

### 1.3. Amide bond formation

As the importance of sustainable practices continues to grow, significant efforts are made to improve the environmental profile of amidation reactions, which constitute approximately 16 % of all reactions employed in the pharmaceutical industry.<sup>42</sup> Amide bonds are a ubiquitous structural motif found in both natural and synthetic compounds, ranging from antibiotics to enzymes. The extensive utility of peptide-based drugs and the prevalence of amide containing pharmaceuticals underscore the critical need for efficient and environmentally sustainable amidation methods.<sup>43-46</sup> Traditionally, amidation processes rely on either harsh reaction conditions or involve specific activating reagents and necessitate large amounts of organic solvents, resulting in substantial environmental impact. Notably, approximately 47 % of all amide bond formations are conducted in dimethylformamide (DMF), a solvent associated with significant toxicity concerns. Regulatory bodies have imposed stricter limitations on DMF, targeting to reduce its exposure to a minimum.<sup>46-48</sup> Amidation reactions, despite their extensive use and thorough investigation, remain among the least environmentally sustainable and operationally efficient processes in synthetic chemistry.<sup>49</sup> In recognition of this issue, the ACS Green Chemistry Institute Pharmaceutical Roundtable (GCIPR) identified the development of sustainable amide coupling methodologies as one of the top ten Key Green Chemistry Research Areas in 2018.<sup>15</sup> The formation of amide bonds typically involves the coupling of a carboxylic acid with an amine, necessitating the activation of at least one component. This activation is commonly achieved using bases, anhydrides, or stoichiometric amounts of coupling reagents, providing more reactive intermediates.

Developing greener and more efficient methods for these vital transformations is an ongoing priority within green chemistry initiatives, particularly in the pharmaceutical industry.<sup>50</sup>

The introduction of carbodiimide reagents, particularly DCC and EDC (figure 2), marked a significant advancement in amide bond formation, enabling carboxylic acid activation under relatively mild conditions.<sup>51,52</sup> However, their utility is limited by inherent drawbacks, including toxicity and the reliance on benzotriazole-based activators to enhance reaction rates and minimize epimerization. These benzotriazole derivatives were designated as class 1 explosives over two decades ago, severely restricting their scalability due to safety concerns.<sup>52,53</sup> In response to these limitations, oxime-based activators, such as Oxyma (2-cyano-2-(hydroxyimino)-acetate), have gained prominence as safer and more efficient alternatives. Oxyma offers significant advantages, including strong racemization suppression and enhanced coupling efficiency, making it highly effective in both manual and automated synthesis.<sup>52,54-56</sup> Building on Oxyma's strengths, the development of COMU, a third generation uronium-type coupling reagent based on Oxyma and a morpholino carbon skeleton, represents a further refinement in coupling methodologies. COMU enhances coupling efficiency, minimizes epimerization, and reduces associated safety hazards. Additionally, COMU's performance is optimized with the use of just one equivalent of base, and its activation process can be conveniently tracked via a distinct color change to yellow, providing a practical and efficient solution for modern amidation processes.<sup>52,55</sup>

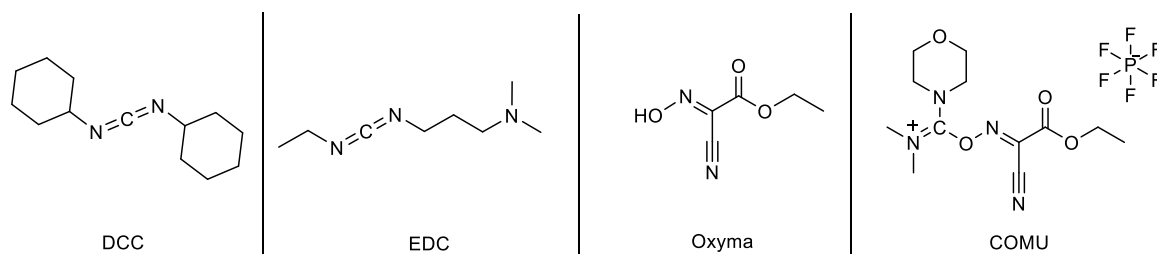


Figure 2: Structures of DCC, EDC, Oxyma and COMU

An environmentally sustainable method for amide bond formation paved the way several years ago, employing an aqueous micellar medium at room temperature. This innovative green method employed the designer surfactant TPGS-750-M, the coupling reagent COMU, and 2,6-lutidine as the base.<sup>52,54</sup> Since this trailblazing report, numerous research teams have built up on these cognitions, extending the scope of water-based amidation reactions under micellar conditions or utilizing HPMC as a surfactant medium. These advancements have facilitated the development of milder, more sustainable conditions in line with green chemistry principles.<sup>36,53-58</sup> Surfactant-based reactions have traditionally been carried out in batch processes, where mixing and mass transfer are dependent on the batch size. However, scaling up these processes presents significant challenges. The use of surfactants typically results in the formation of colloidal suspensions that create slurries (biphasic mixtures), which can impede mass transfer and, as a result, decrease reaction rates.<sup>23,26,33,59</sup>

#### 1.4. Continuous flow chemistry

Continuous flow chemistry provides a highly efficient approach for handling multiphasic reaction mixtures, particularly at larger scales, and has grown substantially over the last decades due to the numerous advantages it provides. Key characteristics of flow chemistry, such as the small channel dimensions and the resulting large surface to volume ratio, enable outstanding heat and mass transfer.<sup>60,61</sup> Additionally, flow chemistry facilitates the safe processing of hazardous reagents and easily accommodates high-temperature and high-pressure conditions. The precise control over reaction parameters ensures high yields and excellent chemo- and regioselectivity. Moreover, process intensification and scale-up are more straightforward in flow chemistry compared to traditional batch processes.<sup>60-65</sup>

The exceptional mixing capabilities of flow reactors make them highly effective for handling biphasic reaction mixtures. While managing liquid-liquid and gas-liquid mixtures under flow conditions is well-established, solid-liquid systems remain more challenging. When non-soluble solids are formed during the reaction or when components are introduced as solid reagents, issues such as clogging and particle settling can frequently occur. These accumulations may cause pressure build-up within the reactor, compromising both process efficiency and operational safety. To address this, active mixing devices specifically designed for solid handling offer a practical solution.<sup>61,63,65</sup> As a result, numerous reactor designs have been developed to manage the complexities of solid-liquid biphasic mixtures, enhancing both safety and operational effectiveness.<sup>66,67</sup>

A remarkable achievement in engineering is the development of spinning disc reactors (SDRs), such as the SpinPro, which handles solids efficiently but simultaneously offers enhanced process control compared to conventional reactor systems.<sup>65,68,69</sup> This reactor features a stationary casing connected to a motor that drives three rotating discs at high velocities. The rapid rotation generates high shear forces, preventing clogging and ensuring efficient mixing of reactants. This results in exceptionally high mass transfer rates, allowing reactions to occur within seconds. The combination of precise temperature control and superior mass transfer enables reactions to proceed under intensified conditions, making the spinning disc reactor particularly effective in terms of production efficiency, safety, and operational flexibility.

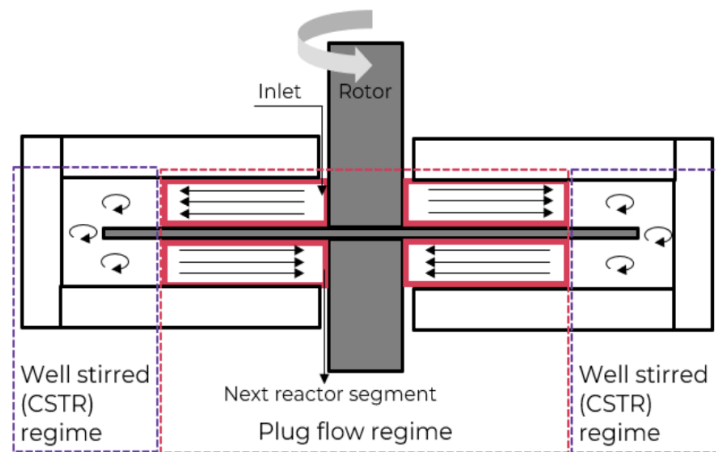


Figure 3: Simplified representation of a single disc of the SpinPro R10.<sup>64</sup>

The advanced rotor-stator spinning disc technology of the SpinPro R10 incorporates three rotating silicon carbide discs (rotors) within a narrow chamber (stator). Silicon carbide is selected for its chemical inertness and corrosion resistance, providing exceptional durability even under harsh conditions. A notable feature of the SpinPro R10 is its dual mixing regimes: plug flow and CSTR. As shown in figure 3, switching between these regimes minimizes backmixing. Intense shear forces in the CSTR zone, combined with the substantial velocity gradient across the 0.5 mm rotor-stator gap, create micro-mixing zones with small vortices. This facilitates Reynolds numbers exceeding  $10^6$ , ensuring superior mixing and efficient mass transfer, further underscoring the reactor's high efficiency.<sup>65,69,70</sup>

## 2. Experimental

### 2.1. Materials and general information

All solvents and chemicals were obtained from typical commercial vendors (TCI, Thermofisher or BLDpharm) and were used as received, without any further purification. Hydroxypropyl methylcellulose (HPMC) was obtained from Gustav Parmentier GmbH (Frankfurt, Germany) in different variants (Mantrocel® E5, E6, E15, E50 and K4M).

$^1\text{H}$ - and  $^{13}\text{C}$ -NMR spectra were recorded on a Bruker Avance III 300 MHz instrument at room temperature (RT), in  $\text{CDCl}_3$  or  $\text{DMSO-d}_6$  as a solvent, at 300 MHz and 75 MHz, respectively. Chemical shifts ( $\delta$ ) are expressed in ppm downfield from TMS as an internal standard. Coupling constants are given in Hz units. The letters s, d, t, q, and m are used to indicate singlet, doublet, triplet, quadruplet, and multiplet, respectively.

Analytical HPLC measurements were carried out on a C18 reversed-phase column ( $150 \times 4.6$  mm, particle size  $5 \mu\text{m}$ ) at  $37^\circ\text{C}$  using mobile phases A [ $\text{H}_2\text{O}/\text{CH}_3\text{CN}$  90:10 (v/v) + 0.1 % TFA] and B ( $\text{CH}_3\text{CN}$  + 0.1 % TFA) at a flow rate of  $1.5 \text{ mL min}^{-1}$ . The following gradient was applied: linear increase from 3 % solution B to 30 % B in 7 min, linear increase from 30 % B to 100 % B in 1 min, hold at 100 % for 1 min. All samples were prepared in HPLC-grade acetonitrile and analyzed at 215 nm via UV-VIS.

GC-MS analysis was performed using a Shimadzu GCMS-QP2010 SE, using an RTX-5MS column ( $30 \text{ m} \times 0.25 \text{ mm} \times 0.25 \mu\text{m}$ ) and helium as carrier gas ( $40 \text{ cm/sec}$  linear velocity). The injector temperature was set to  $280^\circ\text{C}$ . After 1 min at  $50^\circ\text{C}$ , the oven temperature was increased by  $25^\circ\text{C/min}$  to  $300^\circ\text{C}$  and then kept at  $300^\circ\text{C}$  for 3 min. The mass detector was a quadrupole with pre-rods and electron impact ionization. The following settings were used in the detector: ion source temperature  $200^\circ\text{C}$ , interface temperature  $310^\circ\text{C}$ , solvent cut time 2 min 30 sec, acquisition mode scan, mass range  $m/z = 50$  till  $m/z = 400$ .  $100 \mu\text{L}$  of the crude reaction mixture was quenched in 1 mL ethyl acetate and 0.5 mL sodium sulfate. Then,  $100 \mu\text{L}$  of the organic layer was diluted with 1 mL of acetonitrile (HPLC grade) and the content of the vial was then directly analyzed via GC-MS.

Viscosity of HPMC solutions were measured using a Paar Physica UDS 200 universal dynamic rheometer (purchased at Anton Paar) equipped with a MK22 ( $50 \text{ mm}$ ,  $1^\circ$ ) cone at different temperatures. The shear rate was continuously increased over time from  $1 \text{ s}^{-1}$  to  $1000 \text{ s}^{-1}$  in the case of all HPMC E-type solutions, and from  $0.01 \text{ s}^{-1}$  to  $1000 \text{ s}^{-1}$  in the case of HPMC-K4M solutions.



## 2.2. Preparation of HPMC solutions

For the preparation of 100 mL of a 2wt% HPMC/H<sub>2</sub>O solution 66 mL of HPLC-grade water (VWR) were heated to 70 °C under continuous stirring. While stirring at 70 °C, 2.0 g of HPMC Mantrocel® E5 were added, resulting in a turbid solution. The remaining 34 mL of water were added and the solution was allowed to cool to room temperature. While the solution is cooling down, the 2 wt% HPMC/H<sub>2</sub>O solution is getting increasingly clearer until its fully transparent at room temperature. The same procedure can be followed for a 1 wt% and 5 wt% HPMC/H<sub>2</sub>O solution, no matter which HPMC type is used (E5, E6, E15, E50 or K4M).

## 2.3. Residence time distribution study

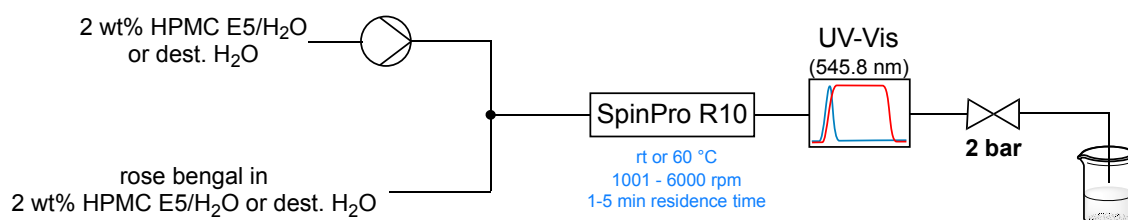
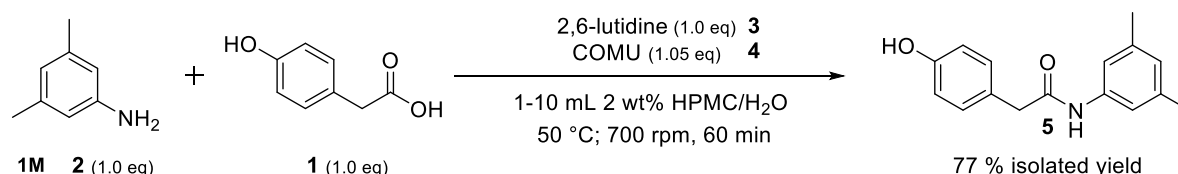


Figure 4: Illustration of the reactor setup used in the RTD studies.

The Residence time distribution (RTD) in the SpinPro R10 reactor (internal volume 19 mL) was investigated using rose bengal ( $c = 500 \mu\text{M}$ ) as a tracer. The studies were performed in distilled water and in 2 wt% HPMC/H<sub>2</sub>O as solvents, whereby 1 mL dye was injected via a 6-port-valve between the pump and reactor. The concentration of the dye at the outlet of the reactor was measured by in-line UV-VIS at 545.8 nm using Avantes Starline AvaSpec-2048 spectrometer with an Avantes AvaLight-DHc lamp as a light source. The recorded spectra were evaluated using Avasoft 8.7 software.

## 2.4. General batch procedure using COMU as coupling reagent



**Scheme 1:** Synthesis of product **1** with COMU as coupling reagent in 2 wt% HPMC/H<sub>2</sub>O. **1** (1 M, 10 mmol) and **B** (1 eq, 1 M) and the organic base 2,6-lutidine (1 eq, 1 M) are equimolar, coupling reagent COMU is in a slight excess of 1.05 eq (10.5 mmol, 1.05 M). Quenching with aq. sat. Na<sub>2</sub>SO<sub>4</sub> and EtOAc.

Substrate **1** (1 M, 10 mmol, 152.15 g/mol) was weighed into a glass vial with screw cap (or round-bottom flask) equipped with a magnetic stirring bar and the solvent HPMC/H<sub>2</sub>O (2 wt%, 1-10 mL). After stirring the suspension for 5 minutes at 50 °C, the addition of the base 2,6-lutidine (1 eq., 10 mmol, 107.15 g/mol) caused the suspension to become a clear solution after a few minutes of stirring. After the mixture got fully clear, adding substrate **2** (1 eq, 10 mmol, 121.18 g/mol) caused the mixture to become a suspension again. Afterwards, the coupling reagent COMU (1.05 eq, 10.5 mmol, 428.27 g/mol) was added and the reaction mixture turned yellowish after a few minutes, indicating the start of the reaction. The reaction mixture was stirred at 50 °C for 60 minutes or until full consumption of the substrates, which was observed via TLC (hexane/EtOAc 3:2, R<sub>f</sub> = 0.45). The progress of the reaction was also monitored by HPLC-UV/VIS. After full conversion, the reaction was quenched with EtOAc and aq. sat. Na<sub>2</sub>SO<sub>4</sub> (each same amount as solvent, 1-10 mL) and the resulting triphasic mixture got stirred for 10 minutes. Then, the precipitated HPMC was removed via filtration through a frit and the remaining organic and aqueous layers were transferred into a separation funnel. The extraction of the base was performed with 3x 1 M HCl (same amount as solvent) and the decomposition product **7** of COMU was removed with 3x aq. sat. Na<sub>2</sub>CO<sub>3</sub> (10x the amount of solvent, until aqueous layer not yellow anymore). The organic layer was dried over Na<sub>2</sub>SO<sub>4</sub> and concentrated via rotary evaporator at 200 mbar. Since the other decomposition product **6** of COMU was not removed with this procedure, washing the dry mixture with DCM is necessary for a **77 %** isolated yield of pure product **5** (1.96 g pure white for 10 mL batch).. Checked and verified with NMR-Data compared to literature (figures 18-19).<sup>53</sup>

**<sup>1</sup>H NMR (300 MHz, DMSO-*d*<sub>6</sub>)**  $\delta$ : 9.90 (s, 1H), 9.26 (s, 1H), 7.21 (d, J = 1.6 Hz, 2H), 7.16 – 7.07 (m, 2H), 6.75 – 6.63 (m, 3H), 3.46 (s, 2H), 2.21 (s, 6H).

**<sup>13</sup>C NMR (75 MHz, DMSO)**  $\delta$ : 169.53, 156.03, 139.17, 137.62, 129.96, 126.22, 124.65, 116.86, 115.07, 42.62, 21.11.

## 2.5. Continuous flow reactor setup

The main reactor module used was a commercially available spinning disc reactor (SpinPro R10, Flowid, Netherlands), designed for mL/min scale and scalability potential.<sup>69</sup> In the flow setup (illustrated in figure 5), standard PFA tubings (0.8 mm or 1.6 mm i.d.), PEEK and stainless-steel Swagelok® fittings and Y-pieces were used. For pumping clear substrate or solvent solutions, Syrris Asia syringe pumps equipped with 1/0.5 mL or 5/2.5 mL syringes or Knauer HPLC pumps (50 mL pump head) were used in combination with check valves (Upchurch, CV-3321) and built-in pressure sensors. For pumping the substrate suspensions, Vapourtec SF-10 pumps equipped with 'blue' peristaltic tubing and built-in pressure sensors were used. Vapourtec SF-10 pumps can provide flow rates from 0.02 mL/min up to 10 mL/min. These pumps are able to pump light slurries and suspensions at pressures up to 10 bar. Since the SpinPro R10 is set for a maximum of 10 bar internal pressure, the pressure limit of the syringe pumps and the Vapourtec pumps were set to 9 bar, for safety reasons.<sup>65</sup> Prior to using the pumps, they were calibrated by pumping water for a specific time and checking the mass balance. Also, a back-pressure regulator (Swagelok) adjusted to 2 bar was used.

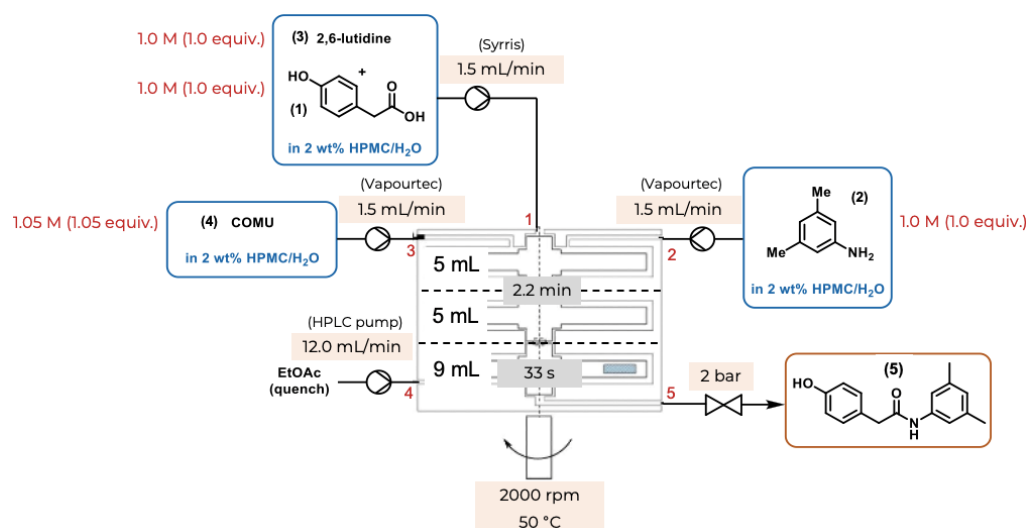


Figure 5: Schematic representation of the continuous flow setup for the synthesis of product 1 with COMU in the SpinPro R10 reactor.

All solutions or suspensions were prepared in 2 wt% HPMC-E5/H<sub>2</sub>O as solvent. Substrates 1 and 3 were combined in one feed. This clear solution was introduced at inlet 1 into the SpinPro R10. At inlet 2, substrate 2 was introduced into the reactor, and 4 at inlet 3. Those two reactants had to be pumped via peristaltic pumps because they form slurry mixtures in 2 wt% HPMC-E5/H<sub>2</sub>O. The amidation was performed using the first two segments of the reactor as reaction zone (with top and middle each having 5 mL of internal volume). At inlet 4, EtOAc was pumped into the reactor as a quench stream (with the bottom segment having 9 mL internal volume) and at outlet 5, the reaction mixture was leaving the reactor. The outlet tubing was connected to a Swagelok-BPR (2 bar reaction pressure) and the mixture was collected in 500 mL Erlenmeyer flasks.

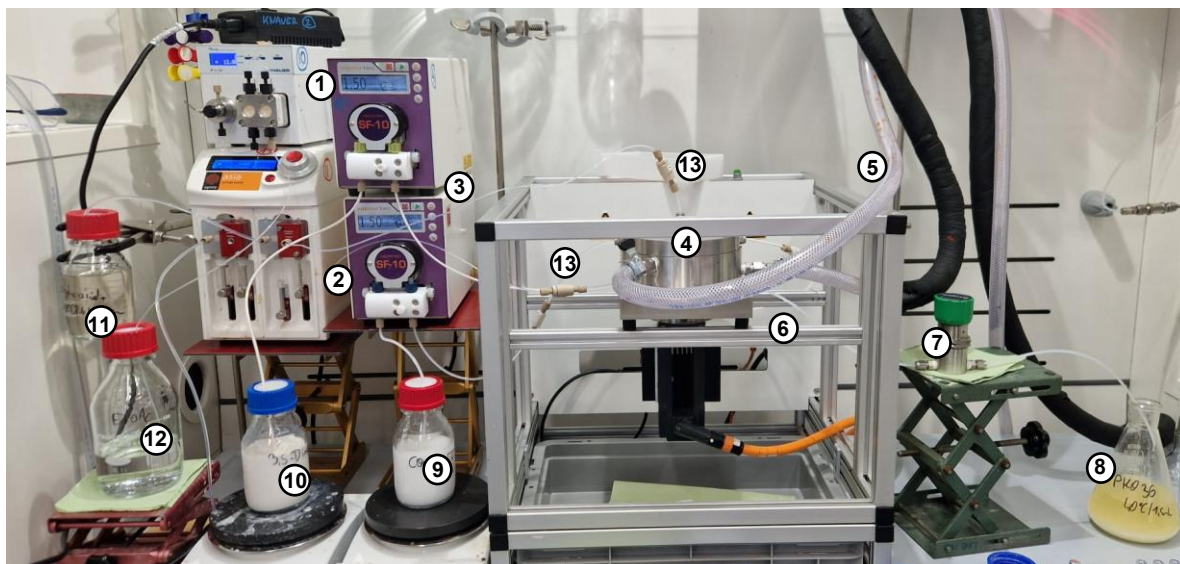


Figure 6: Setup for the synthesis of **1** with COMU in the SpinPro R10 reactor. 1 – HPLC pump, 2 – syringe pump, 3 – peristaltic pumps, 4 – SpinPro R10 reactor, 5 – tubing to the thermostat, 6 – outlet tubing, 7 – BPR (Swagelok), 8 – collection flask, 9 – 1.05 M COMU in 2 wt% HPMC/H<sub>2</sub>O, 10 – 1 M 4-hydroxyphenyl acetic acid + 1 M 2,6-lutidine in 2 wt% HPMC/H<sub>2</sub>O, 11 – 1 M 3,5-dimethylaniline in 2 wt% HPMC/H<sub>2</sub>O, 12 – EtOAc, 13 – check valves.

## 2.6. General procedure for reactions in flow

All feed solutions were prepared in Duran® bottles. *Example substrate feed preparation for a 1 h run:* Feed 1: 4-hydroxyphenyl acetic acid (15.21 g, 1 M, 10 mmol) and 2,6-lutidine (10.72 g, 11.58 mL, 10 mmol) were dissolved in 2 wt% HPMC/H<sub>2</sub>O (100 mL). Feed 2: 3,5 dimethylaniline (12.12 g, 12.47 mL, 10 mmol) was dissolved in 2 wt% HPMC/H<sub>2</sub>O. Feed 3: COMU (44.97 g, 10.5 mmol) was dissolved in 2 wt% HPMC/H<sub>2</sub>O. Feed 2 and 3 were suspensions, delivered via peristaltic pumps. Quench feed: Feed 4: EtOAc.

Setup is shown in figure 3. When the pumps were not in use, the tubings and the pumps were stored under distilled water or in iPrOH in case storage is longer than one week (for compatibility reasons). Before starting the experiments, the pumps, the tubings and the reactor were flushed with water for at least 15 min at a flow rate of 5 mL/min. During the flushing, the thermostat was set to the process temperature of 50 °C and the spinning speed was set to 2000 rpm.

Feeds 1, 2 and 3 were set to a flow rate of 1.5 mL/min (1 eq each). Quench feed was set to a flow rate of 12 mL/min. After 2 min of pumping with an overall flow rate of 16.5 mL/min, sampling was started with fractions taken every 2 minutes. The samples were quenched in 0.5 mL Na<sub>2</sub>SO<sub>4</sub>, then 100 µL of the organic layer of the quenched mixture were dissolved in 1 mL HPLC-grade acetonitrile and measured via HPLC-UV/VIS at 215 nm.

### 3. Results and Discussion

#### 3.1. Characterization of aqueous HPMC mixtures

At the start of this project, experiments were performed to examine the physical properties of aqueous HPMC solutions as potential reaction media. As noted in the introduction, these properties are strongly influenced by the substitution pattern of the methoxy and hydroxypropyl groups in the HPMC polymer.<sup>39,40</sup> The viscosity of these solutions is particularly important when evaluating their suitability for flow process applications. To verify the consistency of the prepared HPMC/H<sub>2</sub>O solutions, routine viscosity measurements were performed. Additionally, to understand how these solutions behave under potential reaction conditions, viscosity was measured at 25 °C, 40 °C, and 60 °C. The variants of HPMC available to us, E5, E6, E15, E50 and K4M, were analyzed as 2 wt% aqueous solutions and summarized in table 1.

Table 1: Results of viscosity measurements of the aqueous HPMC solutions at different temperatures.

No.	Temperature [°C]	Viscosity [mPa*s]						
		Water	E5	E6	E15	E50	K4M	
1	25.3	0.98	4.2	5.3	13.9	26.4	423.2 <sup>a</sup>	4460.3 <sup>b</sup>
2	40.1	0.73	2.8	3.5	8.7	22.5	454.2 <sup>a</sup>	3488.1 <sup>b</sup>
3	60.0	0.64	2.7	3.0	6.8	11.9	285.7 <sup>a</sup>	1106.6 <sup>b</sup>
<sup>a</sup> Eta 1000 value (highest shear rate) <sup>b</sup> Eta 0 value (lowest shear rate)								

The HPMC-variant K4M, which has a slightly lower degree of methoxy substitution compared to the E-types (19-24 % vs. 28-30 %), generated a significantly more viscous aqueous solution, even when used at considerably lower weight percentages.<sup>37,39</sup> The 2 wt% HPMC-K4M/H<sub>2</sub>O solution with a viscosity of 4460 mPa·s at room temperature (25 °C) was excessively viscous, making it unsuitable as a potential reaction medium for flow conditions. Also, HPMC-types E15 and E50 were not chosen as a reaction medium because they were still too viscous. The variants E5 and E6 showed more satisfying results, not only at room temperature but also at 40 °C and 60 °C. As expected and shown in table 1, increasing the temperature led to a decrease in viscosity making these two variants excellent candidates as potential reaction media. Since HPMC-E5 is the most cost effective and most widely available HPMC variant, only this type was used for the flow process development. An example for an average viscosity measurement is illustrated in figure 7, with the remaining ones in appendix (figure 13-14).

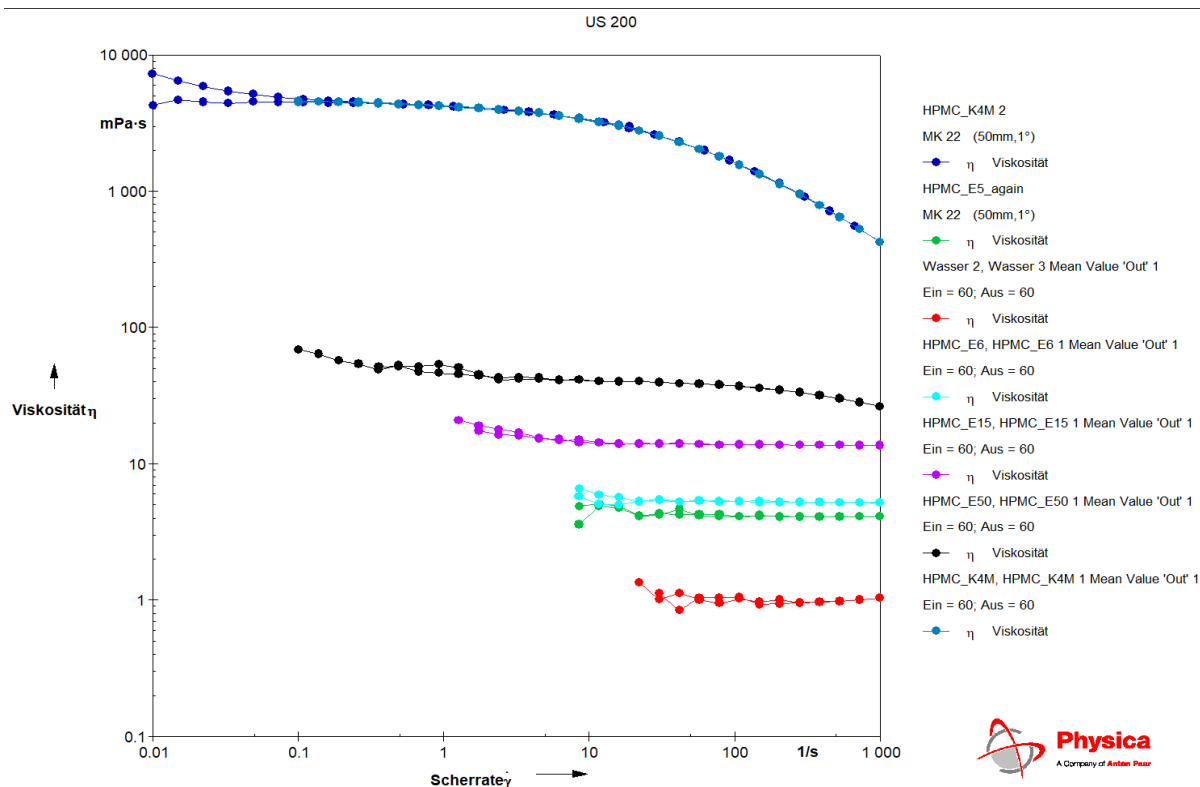
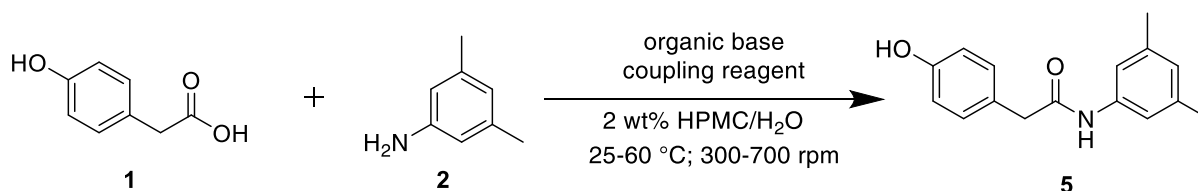


Figure 7: Average viscosity measurement of 2 wt% HPMC/H<sub>2</sub>O solutions at 25 °C. The variants of HPMC investigated are Mantrocel® E5, E6, E15, E50 and K4M.

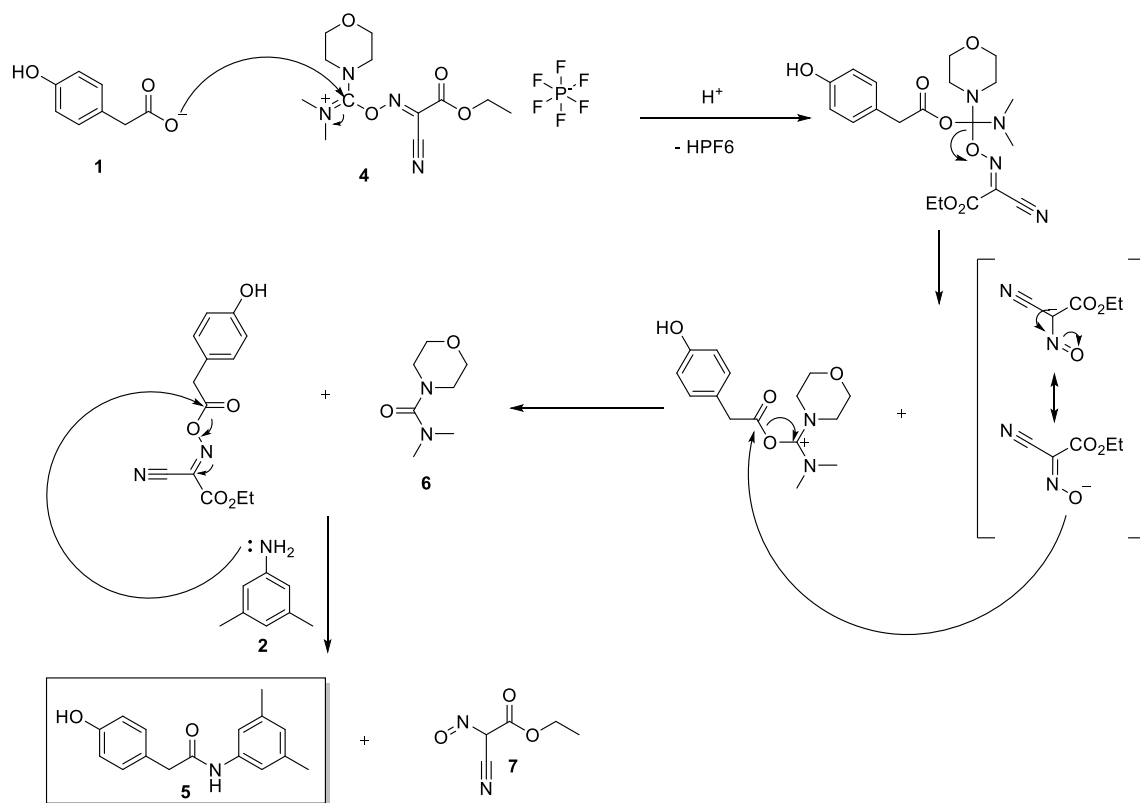
### 3.2. Preliminary batch experiments



Scheme 2: General preparation of product **5** in 2 wt% HPMC/H<sub>2</sub>O.

To explore the impact of HPMC as a surfactant on a water-based amide coupling, a model reaction was selected and analyzed to optimize various reaction parameters and to provide a basis for the flow process development. Illustrated in scheme 2, the starting materials **1** and **2** react in the presence of an organic base and a coupling reagent in 2 wt% HPMC/H<sub>2</sub>O as the solvent to form the desired product **5**, a key intermediate in the production of efaproxiral. Efaproxiral is a pharmacologically significant compound with applications as a lipid-lowering agent and therapeutic potential for conditions such as depression, cancer, traumatic brain injury, ischemia, stroke, myocardial infarction, diabetes, hypoxia, sickle cell disease, hypercholesterolemia, and as a radiosensitizer.<sup>71-73</sup>

COMU **4**, a well-established coupling reagent commonly used in amidation reactions, was employed alongside 2,6-lutidine **3** as the base. This combination, as demonstrated in prior studies, achieved the best results in terms of conversions.<sup>54</sup>



*Scheme 3: Proposed arrow pushing mechanism from literature for amide bond formation with COMU **4** as coupling reagent in a basic milieu.*

The reaction mechanism, illustrated in scheme 3, involves the enhanced reactivity of carboxylate **1** under basic conditions, facilitating the formation of an unstable ketal intermediate with COMU **4** that rapidly decomposes to produce the ester derivative. The separated carbanion delocalizes its negative charge onto the nitroso group, enabling an intermolecular attack on the carbonyl carbon, which results in the elimination of by-product **6**. Finally, nucleophilic attack by xylidine-derivate **2** produces the desired product **5**, accompanied by the formation of by-product **7**.<sup>74</sup>

The first and most important parameter investigated was stirring speed. Most reactions involving HPMC/H<sub>2</sub>O as solvent typically result in the formation of sticky slurries, making efficient mass transfer a critical factor for achieving a successful outcome. Therefore, various batch experiments were conducted at room temperature utilizing 300 rpm, 400 rpm, 500 rpm and 700 rpm. The results are shown in table 2.

Table 2: Effects of the stirring rate with different HPMC variants in 1 mL scale batch reactions.

No. <sup>a</sup>	HPMC variant	time [min]	300 rpm		400 rpm		500 rpm		700 rpm	
			conv. <sup>b</sup>	select. <sup>c</sup>	conv. <sup>b</sup>	select. <sup>c</sup>	conv. <sup>b</sup>	select. <sup>c</sup>	conv. <sup>b</sup>	select. <sup>c</sup>
1	E5	5	40	>95	54	>95	31	>95	69	>95
2		15	30	>95	78	>95	60	>95	76	>95
3		60	35	>95	93	>95	85	>95	85	>95
4	E6	5	n.d. <sup>d</sup>	n.d. <sup>d</sup>	n.d. <sup>d</sup>	n.d. <sup>d</sup>	91	>95	51	>95
5		15					43	>95	54	>95
6		60					84	>95	81	>95
7	E15	5	n.d. <sup>d</sup>	n.d. <sup>d</sup>	n.d. <sup>d</sup>	n.d. <sup>d</sup>	38	>95	78	>95
8		15					53	>95	73	>95
9		60					70	>95	78	>95
10	E50	5	n.d. <sup>d</sup>	n.d. <sup>d</sup>	n.d. <sup>d</sup>	n.d. <sup>d</sup>	71	>95	82	>95
11		15					48	>95	82	>95
12		60					>99	>95	95	>95

<sup>a</sup> 0.72 M of **2**, 0.8 M of **1**, 1.09 M of **3**, 0.76 M of **4** in a 1 mL scale at 25 °C for 1 h. <sup>b</sup> Consumption of starting material, based on HPLC-UV/VIS area% at 215 nm. <sup>c</sup> Selectivity, determined by HPLC-UV/VIS area% at 215 nm. <sup>d</sup> stirring was not possible.

Besides HPMC-E5, stirring rates below 500 rpm always resulted in a mixture that was too viscous to process, causing the stirrers to get stuck and unable to stir (see table 2). At 500 rpm, stirring was possible with all HPMC-variants and the conversions after 60 minutes were promising. In addition, increasing the stirring rate to 700 rpm led to even higher conversions, highlighting the critical role of mass transfer in such slurries. However, processability is also a key factor for the flow process. For all of the HPMC variants investigated, processability at room temperature was identically good, with the slurry formation taking place approximately 1 min after COMU was added. The resulting slurry was sticky but did not affect the reaction at higher stirring speeds.

Based on these observations, all subsequent batch reactions were carried out at 700 rpm to ensure improved homogeneous mixing of the slurry and therefore better mass transfer. To further optimize the reaction, experiments were performed at increasing temperatures and the results are listed below in table 3.



Table 3: Effects of increasing temperature with different HPMC variants in 1 mL scale batch reactions.

No. <sup>a</sup>	HPMC variant	time [min]	conversion [%] <sup>b</sup>			
			25 °C	40 °C	50 °C	60 °C
1	E5	5	69	84	93	99
2		15	76	99	98	99
3		60	85	99	94	94
4	E6	5	51	81	94	94
5		15	54	95	91	94
6		60	81	99	95	99
7	E15	5	78	85	95	93
8		15	73	97	95	96
9		60	78	99	95	95
10	E50	5	82	92	96	99
11		15	82	95	96	99
12		60	95	93	98	99
13	water	5	78	88	93	95
14		15	85	97	98	95
15		60	86	99	99	95

<sup>a</sup> 0.72 M of **2**, 0.8 M of **1**, 1.09 M of **3**, 0.76 M of **4** in a 1 mL scale at 700 rpm for 1 h. <sup>b</sup> Consumption of starting material, based on HPLC-UV/VIS area% at 215 nm. Selectivity, determined by HPLC-UV/VIS area% at 215 nm, always >95 %.

Table 3 highlights the significant influence of the temperature on the reaction. Higher temperatures accelerates the reaction rate, with almost full conversion within just 5 minutes. Additionally, increasing temperatures improved the homogeneity of the reaction mixtures and therefore enhanced processability. It is important to note that even at 60 °C no by-product was observed. A control experiment using HPLC-grade water without adding any HPMC showed similar conversions (table 3; entry 15) with 86–99 % across different temperatures but the reaction mixture exhibited drastically different characteristics. Upon adding COMU, the mixture initially formed an orange, sticky phase, which transitioned into a yellow, rubbery phase after 10 minutes. This poor processability, combined with the inability of pure water to form a homogeneous slurry with compound **2**, rendered neat water unsuitable for flow processes.

All HPMC variants investigated achieved quite similar results. In this specific case, the problem was not to achieve high conversion and selectivity when using HPMC/H<sub>2</sub>O as reaction media but having conditions that allow good processability. The importance of the temperature and its effect on the homogeneity of the resulting slurry could be proved (table 3), as well as the relevance of mass transfer and thus of stirring itself (table 2). This will be something highly tunable in the upcoming flow experiments with the SpinPro R10.

### 3.3. Work-up strategies for the synthesis of **1** with COMU

Since the work-up also plays a decisive role in a synthetic process, several attempts were made to optimize it. After each step in the work-up, an HPLC measurement was performed to check the content of the product mixture. After 60 minutes, the reaction was quenched with EtOAc and aq. sat. Na<sub>2</sub>SO<sub>4</sub> (the same amount as the solvent) and the resulting triphasic mixture was stirred for 10 minutes. The addition of aq. sat. Na<sub>2</sub>SO<sub>4</sub> caused HPMC to precipitate, which was further removed via filtration through a frit and the remaining organic and aqueous layers were transferred into a separation funnel. The extraction of base **3** was performed with 3x 1 M HCl (same amount as the solvent), then by washing with aq. sat. Na<sub>2</sub>CO<sub>3</sub>, by-product **7** was removed as indicated by the strong yellow coloring of the aqueous phase. This step was performed until the aqueous layer was colorless. The organic layer was dried over anhydrous Na<sub>2</sub>SO<sub>4</sub> and concentrated via rotary evaporator at 200 mbar, resulting in a brownish slushy solid. After GC-MS analysis, it was clear that the brownish impurity still present in the material was decomposition product **6**. To get rid of compound **6** without purification on flash column chromatography, an additional washing procedure was needed. Several solubility tests with different organic solvents were performed as shown in appendix (table 11). The impact on the isolated yield was investigated with the most promising solvents based on these findings as presented in table 4. Out of these solvents, DCM, provided the highest isolated yield of 77 %. An illustration of this step is shown in figure 8. Unfortunately, environmentally more acceptable solvents gave rather moderate yields ranging from 20 % to 45 %.

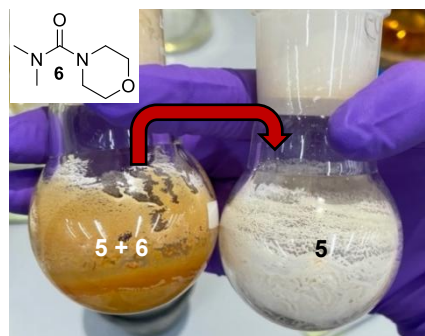


Figure 8: Demonstration of the washing step with DCM.

Table 4: Results for the isolated yields of product **5** with different solvents used in the last step of the work-up.

No.	solvent	isolated yield [%]	solubility	color of product
1	iPrOH	43	~	white
2	EtOAc	45	X	white
3	MeCN	42	X	white
4	DCM	77	X	off white
5	iPrOAc	40	~	white
6	2-Me-THF	20	~	white

In summary, the batch experiments served as a critical preliminary step before transitioning to flow experiments. Understanding the behavior of slurries in water during batch optimization proved essential. Following the successful optimization of key parameters, including work-up conditions, temperature, stirring speed, and thus mass transfer, everything was well-prepared to proceed further with the flow experiments.

### 3.4. Residence time distribution

Before starting reaction parameter optimization in flow, residence time distribution experiments were conducted. Residence time distribution is defined as the probability distribution function which describes the amount of time a fluid element can spend within the reactor. To investigate this, a tracer response technique is employed to understand the fluid behavior within the reactor. The parameters, including rotation speed and residence time, were evaluated, with values provided in table 5.

Table 5: Used parameters for RTD studies.

rotation speed [rpm]	residence time [min]
1000	1
2000	2
3000	3
4000	4
6000	5

RTD was obtained as an exit age distribution function  $[E(t)]$  curve and was calculated with the tracer concentration at the reactor outlet using equation (1).

$$E(t) = \frac{c_{\text{rose bengal}}(t)}{\int_0^{\infty} c_{\text{rose bengal}}(t) dt} \quad (1)$$

The first RTD-studies in the SpinPro R10 were performed in distilled water. Therefore, 1 mL of the tracer solution was injected via a 6-port-valve between the pump and reactor. In this case, the tracer was a dye ( $c = 500 \mu\text{M}$ ) and the concentration of the dye was measured at the outlet of the reactor via absorption by in-line UV-VIS at 545.8 nm. These studies were carried out at fixed rotation speeds but with different flow rates corresponding to different residence times ranging from 1-5 minutes. An example at 2000 rpm is represented in figure 9.

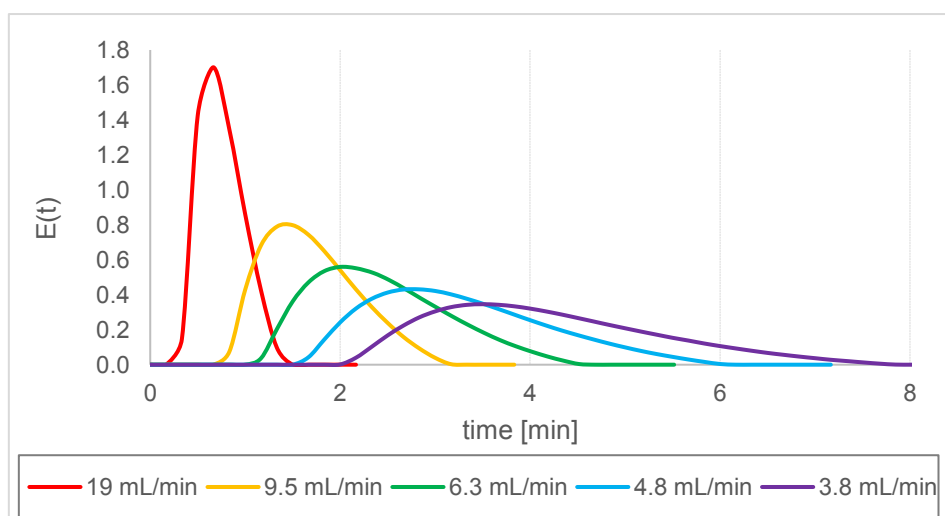


Figure 9: RTD of distilled water at various flow rates and a fixed spinning speed of 2000 rpm at 25 °C in the SpinPro R10.

Figure 9 clearly illustrates that the RTD within the reactor becomes flatter as the flow rate decreases, indicating that longer durations are required for the dye to completely exit the reactor. This trend was consistent across all tested spinning speeds.

Table 6: RTD results for different residence times using distilled water at 25 °C and 2000 rpm in the SpinPro R10.

No. <sup>a</sup>	$t_{\text{theoretical}}$ [min] <sup>b</sup>	flow rate [mL/min]	$\bar{t}$ [min] <sup>c</sup>	Deviation in residence time
1	1.08	19	0.75	30 %
2	2.16	9.5	1.69	21 %
3	3.23	6.3	2.43	25 %
4	4.30	4.8	3.28	24 %
5	5.39	3.8	4.18	22 %

<sup>a</sup> 500  $\mu\text{M}$  of rose bengal. <sup>b</sup> theoretical residence time. <sup>c</sup> mean residence time.

Table 6 shows the values for the determined mean residence times indicating when the majority of the dye leaves the reactor. However, as illustrated in figure 9, it takes longer for the dye to completely leave the reactor. The difference between theoretical residence time and mean residence time is attributed to supplementary system elements, such as the 1 mL sample loop, the 6-port valve and the tubing connecting the reactor outlet to the detector. Both figure 9 and the table 6 highlight that the mean residence times for each curve do not perfectly align with the input values, with deviations between 21 % and 30 %. Lower flow rates than 4.8 mL/min were not evaluated at higher spinning speeds due to the reactor's design, which require a minimum flow rate of 5 mL/min to prevent damage to the fragile reactor discs.<sup>65</sup>

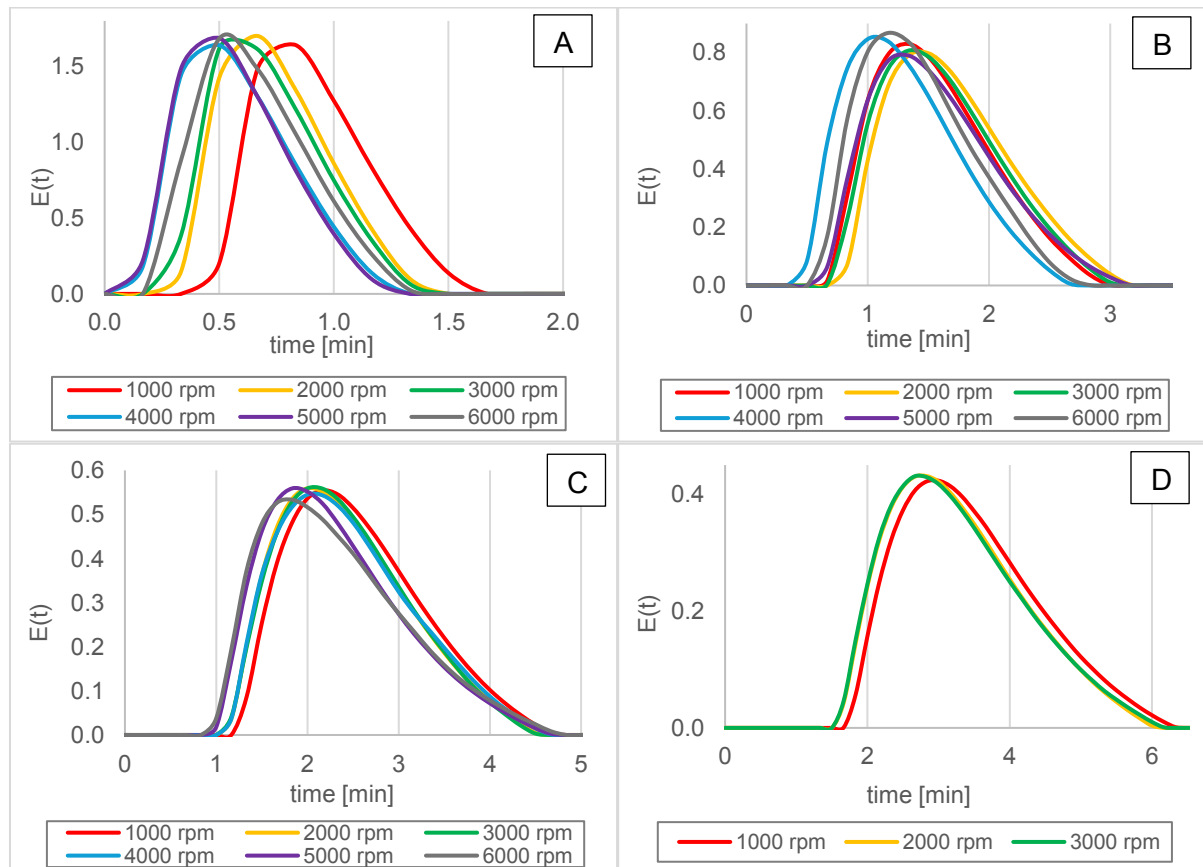


Figure 10: RTD-studies with distilled water in the SpinPro R10 at 25 °C and fixed flow rates with different spinning speeds. A – 19 mL/min; B – 9.5 mL/min; C – 6.3 mL/min; D – 4.8 mL/min.

Figure 10A-D demonstrates that while maintaining constant temperature and flow rate, varying spinning speed had no significant impact on the mean residence time. A slight variation can be observed in 10A at different spinning speeds. This is attributed to the dye solution being flushed out faster at higher spinning speeds. As explained before, the fragile discs require at least 5 mL/min flow rate to prevent damage, so it was not considered safe to apply spinning speeds higher than 3000 rpm at lower flow rates, shown in 10D.

To study the behavior of the medium that will be used for the flow process development, additional experiments were conducted with 2 wt% HPMC-E5. These RTD-studies examined fixed spinning speeds of 1000, 2000, and 4000 rpm and fixed flow rates at two temperatures: 25 °C and 50 °C. As before, 2000 rpm is presented as an example in figure 11. The data corresponding to other spinning speeds is provided in the appendix (see table 13).

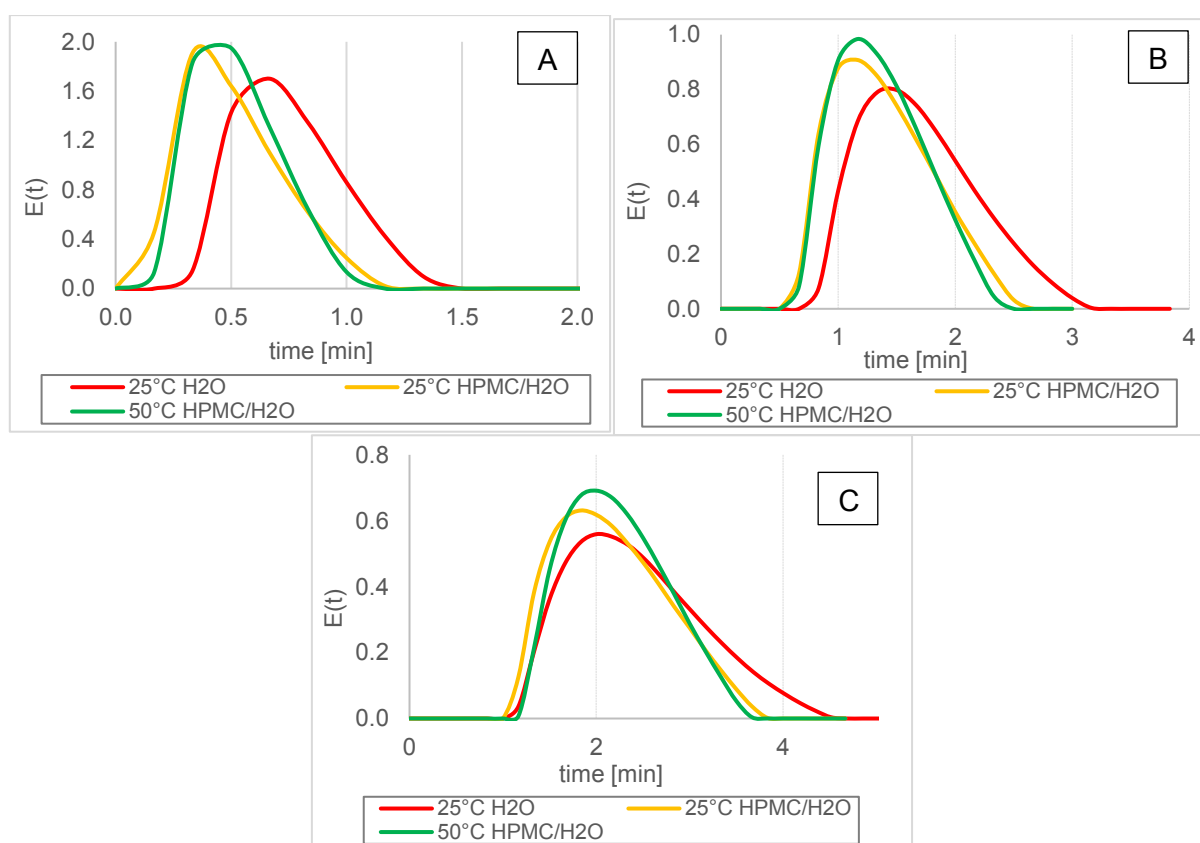


Figure 11: RTD studies for different media in the SpinPro R10 at 2000 rpm.  
A – 19 mL/min; B – 9.5 mL/min; C – 6.3 mL/min

As shown in figure 11A-B, 2 wt% HPMC-E5/H<sub>2</sub>O provides somewhat sharper RTDs than neat water and increasing the temperature did not have a significant impact. However, at a flow rate of 6.3 mL/min (11C), the mean residence time corresponding to both media is almost identical. This tendency remains the same for lower flow rates too. These trends were consistent across all tested spinning speeds and residence times (see appendix, figures 15-16).

### 3.5. Flow process optimization

As the results in batch with COMU as coupling reagent looked promising, several attempts were made to translate the reaction into a flow process using the SpinPro R10 reactor. As the substrates of the model reaction become diluted threefold when entering the reactor (three inlets), they were used in a higher inlet concentrations compared to the batch experiments. Substrate **1** and **3** were combined in feed 1, resulting in a clear solution in 2 wt% HPMC-E5/H<sub>2</sub>O and could therefore be pumped via syringe pump. Substrate **2** (feed 2) and COMU **4** (feed 3) gave milky a suspension in 2 wt% HPMC-E5/H<sub>2</sub>O and was therefore pumped with a peristaltic pump. The first parameter to be optimized using the SpinPro R10 was the spinning speed and in addition, reproducibility tests were also performed simultaneously (table 7).

Table 7: Results for the reproducibility tests of the model reaction performed at different spinning speeds in the SpinPro R10.

<p>all 3 streams prepared in 2 wt% HPMC-E5/H<sub>2</sub>O</p>			
No.	spinning speed [rpm]	conversion <sup>a</sup>	selectivity <sup>b</sup>
1	1000	>82 %	>98 %
2	2000	>91 %	>96 %
3	4000	>74 %	>99 %
4 <sup>c</sup>	1000	>88 %	>99 %
5 <sup>d</sup>	2000	>95 %	>97 %
6 <sup>e</sup>	4000	>90 %	>99 %

<sup>a</sup>Consumption of starting material, based on HPLC-UV/VIS area% at 215 nm. <sup>b</sup> Selectivity, determined by HPLC-UV/VIS area% at 215 nm. <sup>c</sup>rerun of 1. <sup>d</sup>rerun of 2. <sup>e</sup>rerun of 3.

As can be seen in table 7, selectivity was never an issue with all spinning speeds tested. At a spinning speed of 1000 rpm (entry 1) a conversion of over 82 % of the limiting reagent was achieved. When increasing spinning speed to 2000 rpm (entry 2), the conversion raised to over 91 % due to enhanced mass transfer. However, increasing spinning speed further to 4000 rpm (entry 3) caused slight foaming of the outcoming biphasic mixture, resulting in a reduction in conversion. This trend is reproducible (entry 4-6) and the process itself was robust as no clogging occurred during the reaction in the reactor. Based on these studies, 2000 rpm was chosen to be the optimal spinning speed and was used in all the upcoming optimization steps.

The next parameters investigated were the temperature and the residence times (table 8). The impact of the temperature was investigated at 25 °C, 40 °C and 50 °C with fixed flow rates of 1 mL/min for the substrate streams 1-3, and 6 mL/min for the quench feed 4 with EtOAc (entry 1-3). In order to identify the optimal residence time, the experiments were performed at fixed temperatures, as also shown in table 8.

Table 8: Temperature and residence time optimization performed in the SpinPro R10.

<p>all 3 streams prepared in 2 wt% HPMC-E5/H<sub>2</sub>O</p>						
No.	flow rate substrates	flow rate EtOAc	T [°C]	residence time [min]	conversion <sup>a</sup>	selectivity <sup>b</sup>
1	1 mL/min	6 mL/min	25	4min 33 s	>94 %	>99 %
2	1 mL/min	6 mL/min	40		>98 %	>98 %
3	1 mL/min	6 mL/min	50		>99 %	>97 %
4	1.5 mL/min	12 mL/min	40	2min 45s	>95 %	>99 %
5	2 mL/min	15 mL/min	40	2min 10s	>93 %	>98 %
6	<b>1.5 mL/min</b>	<b>12 mL/min</b>	<b>50</b>	<b>2min 45s</b>	<b>&gt;95 %</b>	<b>&gt;97 %</b>
7	2 mL/min	15 mL/min	50	2min 10s	>96 %	>96 %

<sup>a</sup>Consumption of starting material, based on HPLC-UV/VIS area% at 215 nm. <sup>b</sup> Selectivity, determined by HPLC-UV/VIS area% at 215 nm.

By increasing the temperature to 40 °C or 50 °C (entry 2-3), almost complete conversion of substrate **2** could be achieved as shown in table 8. Additionally, steady-state conditions at both temperatures consistently provided high conversions (figures 12 and 17). This stability enabled further exploration and optimization of residence times at these temperatures. An increase of the flow rate by 50 % or 100 % at 40 °C and 50 °C (entry 4-7) had no significant impact on conversion and selectivity. These findings also highlight the robustness, stability and adaptability of the process development in the SpinPro R10 as illustrated in figure 12 as an example corresponding to the reaction in entry 6, table 8. For the optimization of the reactant concentration, it was decided to use 50 °C rather than 40 °C, to counteract possible complications such as clogging.

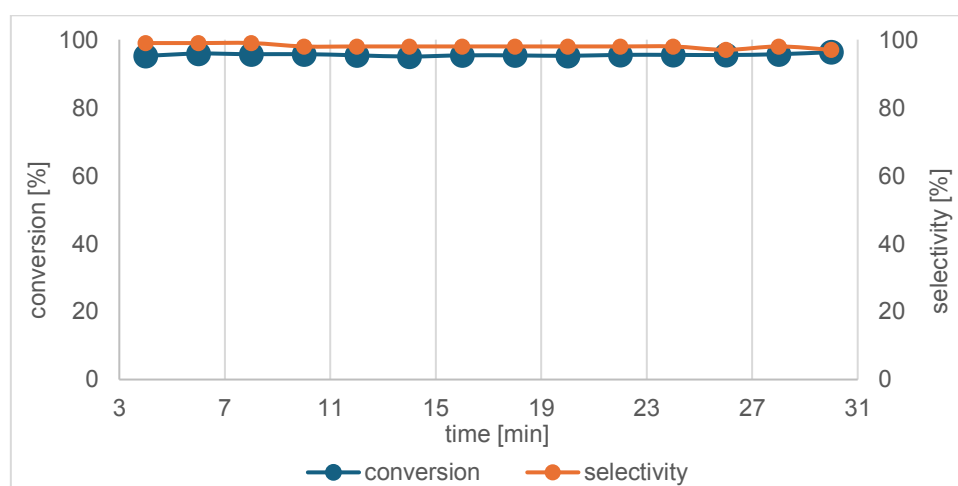


Figure 12: Stability tests for the synthesis of product **5** in the SpinPro R10. Conditions: 2000 rpm, 1.5 mL/min, 50 °C. Samples were collected every 2 min.

Table 9: Results for the concentration optimizations performed in the SpinPro R10.

<p>all 3 streams prepared in 2 wt% HPMC-E5/H<sub>2</sub>O</p>						
No.	$c_2$ [M]	$c_{\text{COMU}}$ [M]	$c_1$ [M]	$c_{\text{Base}}$ [M]	conversion <sup>a</sup>	selectivity <sup>b</sup>
1	1	1.05	1.1	1.5	>95 %	>97 %
2	1	<b>1.05</b>	1	1	<b>&gt;96 %</b>	<b>&gt;98 %</b>
3	1.5	1.575	1.5	1.5	>91 %	>99 %

<sup>a</sup>Consumption of starting material, based on HPLC-UV/VIS area% at 215 nm. <sup>b</sup> Selectivity, determined by HPLC-UV/VIS area% at 215 nm.

With the already established parameters for spinning speed (2000 rpm), temperature (50 °C) and residence time (2.75 min), the last parameter to be optimized was the concentration and ratio of the reactants. Table 9 presents the results of concentration optimization in the SpinPro R10. Gratifyingly, employing 1.0 M concentration, we managed to eliminate the need for any excess in the amount of the base as well as the carboxylic acid, whilst COMU was employed in a slight excess of 1.05 equivalents (entries 1 and 2). Interestingly, using the same equivalents of reactants at a limiting component concentration of 1.5 M (entry 3) resulted in a lower conversion of 91 %, indicating greater slurry formation in the reactor. Additionally, isolation was also performed for those runs, with the highest isolated yield achieved being 77 %, similar to batch. From a green chemistry perspective, minimizing waste is critical. Therefore, the conditions of entry 2, were identified as the optimal parameters, striking a balance between high conversion efficiency and equimolar utilization of substrates.

In summary, the optimized parameters for the synthesis of product **5** in the SpinPro R10 are as follows: Rotation speed (**2000 rpm**), temperature (**50 °C**), residence time (**2.75 min**), flow rates (reactant feeds: **1.5 mL/min**; quench feed: **12 mL/min**) concentrations (COMU **1.05 M**, other reactants **1 M**). With this flow procedure, a theoretical maximum productivity of 22.96 g h<sup>-1</sup> is accessible.



### 3.6. Green metrics

The green metrics were calculated to evaluate the sustainability of the process and the impact on the environment. The E-factor, process mass intensity (PMI), reaction mass efficiency (RME), atom economy (AE), and optimum efficiency (OE) were calculated for the flow process with COMU as coupling reagent using the following equations 2 - 6 from the literature.<sup>75</sup>

$$E\ factor = \frac{\text{total mass of waste}}{\text{mass of product}} \quad (2)$$

$$PMI = \frac{\text{total mass of raw materials used}}{\text{mass of product}} \quad (3)$$

$$RME = \frac{\text{mass of isolated product}}{\text{total mass of reactants}} * 100 \quad (4)$$

$$AE = \frac{\text{molecular weight of product}}{\text{total molecular weight of reactants}} * 100 \quad (5)$$

$$OE = \frac{RME}{AE} * 100 \quad (6)$$

Table 10: Calculated quantitative green metrics for the synthesis of product **5** in the optimized flow process utilizing COMU.

<p>all 3 streams prepared in 2 wt% HPMC-E5/H<sub>2</sub>O</p>	
metric	COMU flow
conversion [%]	>96
yield [%]	77
E-factor	2.25
PMI	3.25
RME [%]	23.7
AE [%]	31.5
OE [%]	75.2

The results, listed in table 10, show quantitative green metrics without considering HPMC in pure water as surfactant and EtOAc as quench in the calculations because of the fact that both components can easily be recovered. The E-factors for pharmaceuticals typically range between 25 and 100 due to the stepwise process of chemical synthesis, providing even higher values for PMI.<sup>57</sup> With an E-factor of 2.25 and a PMI of 3.25, this continuous flow procedure provides product **5** in a greener, more sustainable way.

### 3.7. Conclusion and Outlook

A flow process was developed and optimized for the amidation of 4-hydroxyphenyl acetic acid (**1**) with 3,5-dimethylaniline (**2**), utilizing 2,6-lutidine (**3**) as base and COMU (**4**) as coupling reagent to provide *N*-(3,5-dimethylphenyl)-2-(4-hydroxyphenyl)acetamide (**5**) in 2 wt% HPMC-E5/H<sub>2</sub>O as reaction medium. For that purpose, the physical properties of the 2 wt% HPMC/H<sub>2</sub>O solutions with different HPMC variants were analyzed finding that variants E5 and E6 in particular stood out as excellent candidates for the application as surfactants. Several preliminary batch experiments were performed to investigate the behavior of the sticky slurries as reaction mixtures at different stirring speeds and different temperatures. The conversion gets higher (up to **98 %**) with increasing stirring rates up to 700 rpm and increased temperatures up to 50 °C. Several attempts were made to optimize the last step of the work-up by testing a variation of solvents to selectively wash away by-product **6** without further purification via flash column chromatography. Of all solvents investigated for this purpose, DCM provided the best results with an isolated yield of **77 %** of pure product **5**. Based on the results of the batch reaction data, the flow process was subsequently optimized by adjusting various parameters, including spinning speed of the reactor disk, temperature, residence time, and reactant concentration. During all flow experiments, no technical problems were encountered, which confirmed the robustness of the SpinPro R10 system and its ability to handle slurries. The optimized conditions for the synthesis of product **5** in the SpinPro R10 were as follows: Rotation speed (**2000 rpm**), temperature (**50 °C**), residence time (**2.75 min**), inlet feed concentrations (COMU **1.05 M**, every other reactant **1 M**). With this flow procedure, a theoretical maximum output of 22.96 g h<sup>-1</sup> is accessible. Additionally, this provides an E-factor of 2.25 and a PMI of 3.25.

## 4. References

- (1) Mutlu, H., & Barner, L. (2022). Getting the terms right: green, sustainable, or circular chemistry? *Macromolecular Chemistry and Physics*, 223(13), 2200111. <https://doi.org/10.1002/macp.202200111>
- (2) Green Chemistry and Catalysis: Prof. Dr. Roger Arthur Sheldon, Dr. Isabel W. C. E. Arends, Dr. Ulf Hanefeld DOI:10.1002/9783527611003
- (3) Clark, J. H., Luque, R., & Matharu, A. S. (2012). Green chemistry, biofuels, and biorefinery. *Annual review of chemical and biomolecular engineering*, 3(1), 183-207. <https://doi.org/10.1146/annurev-chembioeng-062011-081014>
- (4) Cernansky, R. (2015). Chemistry: green refill. *Nature*, 519(7543), 379-380. <https://doi.org/10.1038/nj7543-379a>
- (5) Sanderson, K. (2011). Chemistry: It's not easy being green. *Nature*, 469(7328), 18-20. <https://doi.org/10.1038/469018a>
- (6) Poliakoff, M., & Licence, P. (2007). Sustainable technology-Green chemistry. *Nature*, 450(7171), 810-812. <https://doi.org/10.1038/450810a>
- (7) Clark, J. H. (1999). Green chemistry: challenges and opportunities. *Green chemistry*, 1(1), 1-8.
- (8) Sheldon, R. A. (2017). The E factor 25 years on: the rise of green chemistry and sustainability. *Green Chemistry*, 19(1), 18-43. DOI: [10.1039/C6GC02157C](https://doi.org/10.1039/C6GC02157C)
- (9) P. Anastas and J. C. Warner, *Green Chemistry: Theory and Practice*, Oxford University Press, Oxford, 1998. <https://doi.org/10.1093/oso/9780198506980.001.0001>
- (10) Hammer, S., Nanto, F., Canu, P., Ötvös, S. B., & Kappe, C. O. (2024). Application of an Oscillatory Plug Flow Reactor to Enable Scalable and Fast Reactions in Water Using a Biomass-Based Polymeric Additive. *ChemSusChem*, 17(2), e202301149. <https://doi.org/10.1002/cssc.202301149>
- (11) Kitanosono, T., & Kobayashi, S. (2021). Synthetic organic "aqua chemistry" that relies on neither cosolvents nor surfactants. *ACS Central Science*, 7(5), 739-747. <https://doi.org/10.1021/acscentsci.1c00045>
- (12) Lipshutz, B. H., Gallou, F., & Handa, S. (2016). Evolution of solvents in organic chemistry. *ACS sustainable chemistry & engineering*, 4(11), 5838-5849. <https://doi.org/10.1021/acssuschemeng.6b01810>
- (13) Clarke, C. J., Tu, W. C., Levers, O., Brohl, A., & Hallett, J. P. (2018). Green and sustainable solvents in chemical processes. *Chemical reviews*, 118(2), 747-800. <https://doi.org/10.1021/acs.chemrev.7b00571>
- (14) Cortes-Clerget, M., Yu, J., Kincaid, J. R., Walde, P., Gallou, F., & Lipshutz, B. H. (2021). Water as the reaction medium in organic chemistry: from our worst enemy to our best friend. *Chemical science*, 12(12), 4237-4266. <https://doi.org/10.1039/D0SC06000C>
- (15) Bryan, M. C., Dunn, P. J., Entwistle, D., Gallou, F., Koenig, S. G., Hayler, J. D., et. al. (2018). Key Green Chemistry research areas from a pharmaceutical manufacturers' perspective revisited. *Green Chemistry*, 20(22), 5082-5103. <https://doi.org/10.1039/C8GC01276H>
- (16) Henderson, R. K., Jiménez-González, C., Constable, D. J., Alston, S. R., Inglis, G. G., Fisher, G., et. al. (2011). Expanding GSK's solvent selection guide—embedding sustainability into solvent selection starting at medicinal chemistry. *Green Chemistry*, 13(4), 854-862. <https://doi.org/10.1039/C0GC00918K>
- (17) Gao, F., Chang, H., Li, J., Wang, R., & Gu, Y. (2023). Replacing polar aprotic solvents with water in organic synthesis. *Current Opinion in Green and Sustainable Chemistry*, 40, 100774. <https://doi.org/10.1016/j.cogsc.2023.100774>
- (18) Hazra, S., Gallou, F., & Handa, S. (2022). Water: an underestimated solvent for amide bond-forming reactions. *ACS Sustainable Chemistry & Engineering*, 10(16), 5299-5306. <https://doi.org/10.1021/acssuschemeng.2c00520>
- (19) Sharma, S., Das, J., Braje, W. M., Dash, A. K., & Handa, S. (2020). A glimpse into green chemistry practices in the pharmaceutical industry. *ChemSusChem*, 13(11), 2859-2875. <https://doi.org/10.1002/cssc.202000317>
- (20) Kitanosono, T., Masuda, K., Xu, P., & Kobayashi, S. (2018). Catalytic organic reactions in water toward sustainable society. *Chemical reviews*, 118(2), 679-746. <https://doi.org/10.1021/acs.chemrev.7b00417>
- (21) Lipshutz, B. H., & Ghorai, S. (2014). Transitioning organic synthesis from organic solvents to water. What's your E Factor?. *Green Chemistry*, 16(8), 3660-3679. <https://doi.org/10.1039/C4GC00503A>
- (22) Erythropel, H. C., Zimmerman, J. B., de Winter, T. M., Petitjean, L., Melnikov, F., Lam, C. H., et. al. (2018). The Green ChemisTREE: 20 years after taking root with the 12 principles. *Green chemistry*, 20(9), 1929-1961. <https://doi.org/10.1039/C8GC00482J>

- (23) Wernik, M., Sipos, G., Buchholcz, B., Darvas, F., Novák, Z., Ötvös, S. B., & Kappe, C. O. (2021). Continuous flow heterogeneous catalytic reductive aminations under aqueous micellar conditions enabled by an oscillatory plug flow reactor. *Green Chemistry*, 23(15), 5625-5632. <https://doi.org/10.1039/D1GC02039K>
- (24) Hedouin, G., Ogulu, D., Kaur, G., & Handa, S. (2023). Aqueous micellar technology: An alternative beyond organic solvents. *Chemical Communications*, 59(20), 2842-2853. <https://doi.org/10.1039/D3CC00127J>
- (25) La Sorella, G., Strukul, G., & Scarso, A. (2015). Recent advances in catalysis in micellar media. *Green Chemistry*, 17(2), 644-683. <https://doi.org/10.1039/C4GC01368A>
- (26) Lipshutz, B. H. (2017). When does organic chemistry follow nature's lead and "make the switch"? *The Journal of Organic Chemistry*, 82(6), 2806-2816. <https://doi.org/10.1021/acs.joc.7b00010>
- (27) Steven, A. (2019). Micelle-mediated chemistry in water for the synthesis of drug candidates. *Synthesis*, 51(13), 2632-2647.
- (28) Compagno, N., Profeta, R., & Scarso, A. (2023). Recent advances in the synthesis of active pharmaceutical and agrochemical ingredients in micellar media. *Current Opinion in Green and Sustainable Chemistry*, 39, 100729. <https://doi.org/10.1016/j.cogsc.2022.100729>
- (29) Lipshutz, B. H., Ghorai, S., & Cortes-Clerget, M. (2018). The hydrophobic effect applied to organic synthesis: recent synthetic chemistry "in water". *Chemistry—A European Journal*, 24(26), 6672-6695. <https://doi.org/10.1002/chem.201705499>
- (30) Thakore, R. R., Takale, B. S., Hu, Y., Ramer, S., Kostal, J., Gallou, F., & Lipshutz, B. H. (2021). "TPG-lite": A new, simplified "designer" surfactant for general use in synthesis under micellar catalysis conditions in recyclable water. *Tetrahedron*, 87, 132090. <https://doi.org/10.1016/j.tet.2021.132090>
- (31) Lee, N. R., Cortes-Clerget, M., Wood, A. B., Lippincott, D. J., Pang, H., Moghadam, F. A., et al. (2019). Coolade. A Low-Foaming Surfactant for Organic Synthesis in Water. *ChemSusChem*, 12(13), 3159-3165. <https://doi.org/10.1002/cssc.201900369>
- (32) Cortes-Clerget, M., Spink, S. E., Gallagher, G. P., Chaisemartin, L., Filaire, E., Berthon, J. Y., & Lipshutz, B. H. (2019). MC-1. A "designer" surfactant engineered for peptide synthesis in water at room temperature. *Green Chemistry*, 21(10), 2610-2614. <https://doi.org/10.1039/C9GC01050E>
- (33) Lorenzetto, T., Berton, G., Fabris, F., & Scarso, A. (2020). Recent designer surfactants for catalysis in water. *Catalysis Science & Technology*, 10(14), 4492-4502. <https://doi.org/10.1039/D0CY01062F>
- (34) Borlinghaus, N., Ansari, T. N., von Garrel, L. H., Ogulu, D., Handa, S., Wittmann, V., & Braje, W. M. (2021). Nucleophilic aromatic substitution reactions under aqueous, mild conditions using polymeric additive HPMC. *Green Chemistry*, 23(11), 3955-3962. <https://doi.org/10.1039/D1GC00128K>
- (35) Sharma, S., Ansari, T. N., & Handa, S. (2021). HPMC: a biomass-based semisynthetic sustainable additive enabling clean and fast chemistry in water. *ACS Sustainable Chemistry & Engineering*, 9(38), 12719-12728. <https://doi.org/10.1021/acssuschemeng.1c04607>
- (36) Petkova, D., Borlinghaus, N., Sharma, S., Kaschel, J., Lindner, T., Klee, J., et al. (2020). Hydrophobic pockets of HPMC enable extremely short reaction times in water. *ACS Sustainable Chemistry & Engineering*, 8(33), 12612-12617. <https://doi.org/10.1021/acssuschemeng.0c03975>
- (37) Li, C. L., Martini, L. G., Ford, J. L., & Roberts, M. (2005). The use of hypromellose in oral drug delivery. *Journal of pharmacy and pharmacology*, 57(5), 533-546. <https://doi.org/10.1211/0022357055957>
- (38) Borlinghaus, N., Wittmann, V., & Braje, W. M. (2022). Using polymeric hydroxypropyl methylcellulose as an alternative to 'micellar catalysis' to enable chemical reactions in water. *Current Opinion in Green and Sustainable Chemistry*, 33, 100571. <https://doi.org/10.1016/j.cogsc.2021.100571>
- (39) Gustafsson, C., Bonferoni, M. C., Caramella, C., Lennholm, H., & Nyström, C. (1999). Characterisation of particle properties and compaction behaviour of hydroxypropyl methylcellulose with different degrees of methoxy/hydroxypropyl substitution. *European journal of pharmaceutical sciences*, 9(2), 171-184. [https://doi.org/10.1016/S0928-0987\(99\)00054-8](https://doi.org/10.1016/S0928-0987(99)00054-8)
- (40) Nokhodchi, A., Ford, J. L., & Rubinstein, M. H. (1997). Studies on the interaction between water and (hydroxypropyl) methylcellulose. *Journal of pharmaceutical sciences*, 86(5), 608-615. <https://doi.org/10.1021/js960279a>
- (41) Sarkar, N. (1979). Thermal gelation properties of methyl and hydroxypropyl methylcellulose. *Journal of applied polymer science*, 24(4), 1073-1087. <https://doi.org/10.1002/app.1979.070240420>
- (42) Al Musaimi, O., de la Torre, B. G., & Albericio, F. (2020). Greening Fmoc/t Bu solid-phase peptide synthesis. *Green Chemistry*, 22(4), 996-1018. <https://doi.org/10.1039/C9GC03982A>
- (43) Manske, C., Schmiedtchen, M., Gellhaar, S., Kiesel, M., & Becker, J. (2022). Amide and Peptide Couplings Mediated by Pivaloyl Mixed Anhydrides in Aqueous Media. *ACS Sustainable Chemistry & Engineering*, 10(16), 5307-5314. <https://doi.org/10.1021/acssuschemeng.2c00642>

- (44) Manne, S. R., Sharma, A., Sazonovas, A., El-Faham, A., de la Torre, B. G., & Albericio, F. (2022). Understanding OxymaPure as a peptide coupling additive: A guide to new oxyma derivatives. *ACS omega*, 7(7), 6007-6023. <https://doi.org/10.1021/acsomega.1c06342>
- (45) Alfano, A. I., Lange, H., & Brindisi, M. (2022). Amide bonds meet flow chemistry: a journey into methodologies and sustainable evolution. *ChemSusChem*, 15(6), e202102708. <https://doi.org/10.1002/cssc.202102708>
- (46) Dunetz, J. R., Magano, J., & Weisenburger, G. A. (2016). Large-scale applications of amide coupling reagents for the synthesis of pharmaceuticals. *Organic Process Research & Development*, 20(2), 140-177. <https://doi.org/10.1021/op500305s>
- (47) MacMillan, D. S., Murray, J., Sneddon, H. F., Jamieson, C., & Watson, A. J. (2013). Evaluation of alternative solvents in common amide coupling reactions: replacement of dichloromethane and N, N-dimethylformamide. *Green Chemistry*, 15(3), 596-600. <https://doi.org/10.1039/C2GC36900A>
- (48) Sherwood, J., Albericio, F., & de la Torre, B. G. (2024). N, N-Dimethyl Formamide European Restriction Demands Solvent Substitution in Research and Development. *ChemSusChem*, 17(8), e202301639. <https://doi.org/10.1002/cssc.202301639>
- (49) Isidro-Llobet, A., Kenworthy, M. N., Mukherjee, S., Kopach, M. E., Wegner, K., Gallou, F., et.al. (2019). Sustainability challenges in peptide synthesis and purification: from R&D to production. *The Journal of organic chemistry*, 84(8), 4615-4628. <https://doi.org/10.1021/acs.joc.8b03001>
- (50) Todorovic, M., & Perrin, D. M. (2020). Recent developments in catalytic amide bond formation. *Peptide Science*, 112(6), e24210. <https://doi.org/10.1002/pep2.24210>
- (51) Sheehan, J. C., & Hess, G. P. (1955). A new method of forming peptide bonds. *Journal of the American Chemical Society*, 77(4), 1067-1068. <https://doi.org/10.1021/ja01609a099>
- (52) Albericio, F., & El-Faham, A. (2018). Choosing the right coupling reagent for peptides: a twenty-five-year journey. *Organic Process Research & Development*, 22(7), 760-772. <https://doi.org/10.1021/acs.oprd.8b00159>
- (53) Sharma, S., Buchbinder, N. W., Braje, W. M., & Handa, S. (2020). Fast amide couplings in water: Extraction, column chromatography, and crystallization not required. *Organic Letters*, 22(15), 5737-5740. <https://doi.org/10.1021/acs.orglett.0c01676>
- (54) Gabriel, C. M., Keener, M., Gallou, F., & Lipshutz, B. H. (2015). Amide and peptide bond formation in water at room temperature. *Organic letters*, 17(16), 3968-3971. <https://doi.org/10.1021/acs.orglett.5b01812>
- (55) El-Faham, A., & Albericio, F. (2011). Peptide coupling reagents, more than a letter soup. *Chemical reviews*, 111(11), 6557-6602. <https://doi.org/10.1021/cr100048w>
- (56) Subirós-Funosas, R., Prohens, R., Barbas, R., El-Faham, A., & Albericio, F. (2009). Oxyma: An Efficient Additive for Peptide Synthesis to Replace the Benzotriazole-Based HOBt and HOAt with a Lower Risk of Explosion [1]. *Chemistry—A European Journal*, 15(37), 9394-9403. <https://doi.org/10.1002/chem.200900614>
- (57) Cortes-Clerget, M., Berthon, J. Y., Krolkiewicz-Renimel, I., Chaisemartin, L., & Lipshutz, B. H. (2017). Tandem deprotection/coupling for peptide synthesis in water at room temperature. *Green Chemistry*, 19(18), 4263-4267. <https://doi.org/10.1039/C7GC01575E>
- (58) Gallou, F., Buescher, K., Schreiber, R., Durano, C., Parmentier, M., Ye, N., et.al. (2020). Surfactant technology: to new rules, new design required!. *Organic process research & development*, 24, 841-849. <https://doi.org/10.1021/acs.oprd.9b00454>
- (59) Kitanosono, T., Masuda, K., Xu, P., & Kobayashi, S. (2018). Catalytic organic reactions in water toward sustainable society. *Chemical reviews*, 118(2), 679-746. <https://doi.org/10.1021/acs.chemrev.7b00417>
- (60) Akwi, F. M., & Watts, P. (2018). Continuous flow chemistry: where are we now? Recent applications, challenges and limitations. *Chemical communications*, 54(99), 13894-13928. <https://doi.org/10.1039/C8CC07427E>
- (61) Plutschack, M. B., Pieber, B., Gilmore, K., & Seeberger, P. H. (2017). The hitchhiker's guide to flow chemistryII. *Chemical reviews*, 117(18), 11796-11893. <https://doi.org/10.1021/acs.chemrev.7b00183>
- (62) Capaldo, L., Wen, Z., & Noël, T. (2023). A field guide to flow chemistry for synthetic organic chemists. *Chemical science*, 14(16), 4230-4247. <https://doi.org/10.1039/D3SC00992K>
- (63) Gutmann, B., Cantillo, D., & Kappe, C. O. (2015). Continuous-flow technology—a tool for the safe manufacturing of active pharmaceutical ingredients. *Angewandte Chemie International Edition*, 54(23), 6688-6728. <https://doi.org/10.1002/anie.201409318>
- (64) Buglioni, L., Raymenants, F., Slattery, A., Zondag, S. D., & Noël, T. (2021). Technological innovations in photochemistry for organic synthesis: flow chemistry, high-throughput experimentation, scale-up, and photoelectrochemistry. *Chemical Reviews*, 122(2), 2752-2906. <https://doi.org/10.1021/acs.chemrev.1c00332>



- (65) Polteraue, D., van Eeten, K. M., Stam, W., Hone, C. A., & Kappe, C. O. (2024). Dynamic Spinning Disc Reactor Technology to Enable In Situ Solid Product Formation in a Diazotization and Azo Coupling Sequence. *Organic Process Research & Development*, 28(5), 1903-1909. <https://doi.org/10.1021/acs.oprd.3c00448>
- (66) Doyle, B. J., Gutmann, B., Bittel, M., Hubler, T., Macchi, A., & Roberge, D. M. (2019). Handling of solids and flow characterization in a baffless oscillatory flow coil reactor. *Industrial & Engineering Chemistry Research*, 59(9), 4007-4019. <https://doi.org/10.1021/acs.iecr.9b04496>
- (67) Bianchi, P., Williams, J. D., & Kappe, C. O. (2020). Oscillatory flow reactors for synthetic chemistry applications. *Journal of Flow Chemistry*, 10(3), 475-490. <https://doi.org/10.1007/s41981-020-00105-6>
- (68) Mo, Y., & Jensen, K. F. (2016). A miniature CSTR cascade for continuous flow of reactions containing solids. *Reaction Chemistry & Engineering*, 1(5), 501-507. <https://doi.org/10.1039/C6RE00132G>
- (69) Cherkasov, N., Adams, S. J., Bainbridge, E. G., & Thornton, J. A. (2023). Continuous stirred tank reactors in fine chemical synthesis for efficient mixing, solids-handling, and rapid scale-up. *Reaction Chemistry & Engineering*, 8(2), 266-277. <https://doi.org/10.1039/D2RE00232A>
- (70) Hop, C. J. W., Jansen, R., Besten, M., Chaudhuri, A., Baltussen, M. W., & van der Schaaf, J. (2023). Hydrodynamics of a rotor–stator spinning disk reactor: Investigations by large-eddy simulation. *Physics of Fluids*, 35(3). <https://doi.org/10.1063/5.0137405>
- (71) Suh, J. H. (2004). Efaproxiral: a novel radiation sensitiser. *Expert Opinion on Investigational Drugs*, 13(5), 543-550. <https://doi.org/10.1517/13543784.13.5.543>
- (72) Shi, H., Cao, J., & Hu, Y. (2008). Green Synthesis Applicable for Industrial-Scale Preparation of Efaproxiral Sodium. *Industrial & engineering chemistry research*, 47(9), 2861-2866. <https://doi.org/10.1021/ie071279w>
- (73) Kunert, M. P., Liard, J. F., & Abraham, D. J. (1996). RSR-13, an allosteric effector of hemoglobin, increases systemic and iliac vascular resistance in rats. *American Journal of Physiology-Heart and Circulatory Physiology*, 271(2), H602-H613. <https://doi.org/10.1152/ajpheart.1996.271.2.H602>
- (74) Valeur, E., & Bradley, M. (2009). Amide bond formation: beyond the myth of coupling reagents. *Chemical Society Reviews*, 38(2), 606-631. <https://doi.org/10.1039/B701677H>
- (75) Nagy, B. S., Fu, G., Hone, C. A., Kappe, C. O., & Ötvös, S. B. (2023). Harnessing a Continuous-Flow Persulfuric Acid Generator for Direct Oxidative Aldehyde Esterifications. *ChemSusChem*, 16(2), e202201868. <https://doi.org/10.1002/cssc.202201868>

## 5. Appendix

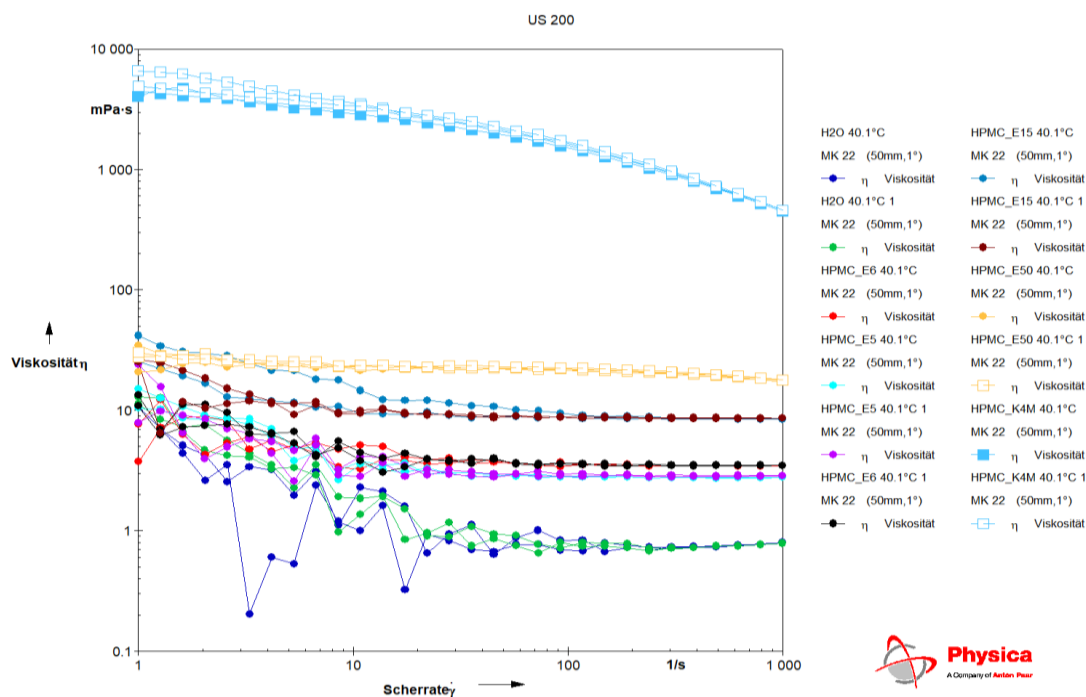


Figure 13: Viscosity measurement of 2 wt% HPMC/H<sub>2</sub>O solutions at 40 °C. The variants investigated of HPMC are Mantrocel® E5, E6, E15, E50 and K4M.

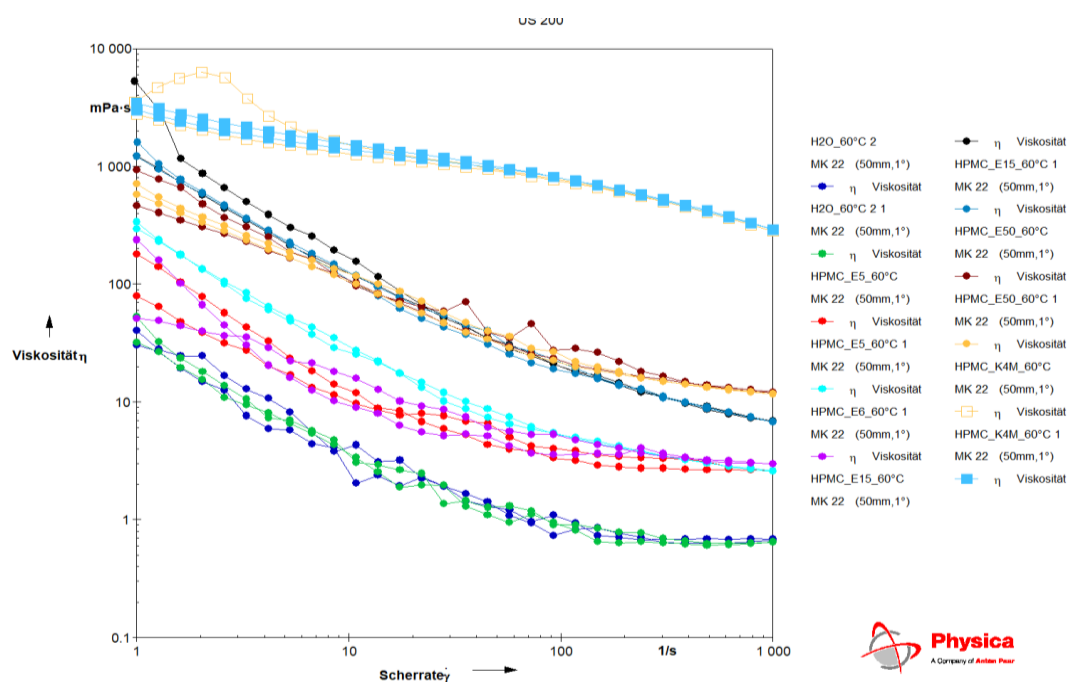


Figure 14: Viscosity measurement of 2 wt% HPMC/H<sub>2</sub>O solutions at 60 °C. The variants investigated of HPMC are Mantrocel® E5, E6, E15, E50 and K4M.

Table 11: Results for solubility tests to remove decomposition product **A** of COMU.

solvent	product	byproduct	notes
DCM	X	✓	not wanted
water	X	X	
EtOH	✓	✓	dissolved product <b>1</b> after 5 min
i-PrOH	~	✓	
n-BuOH	~	~	dissolved product <b>1</b> after 5 min
EtOAc	X	✓	product <b>1</b> is just soluble in excess of EtOAc
acetone	✓	✓	
diethylether	X	X	
ethylene glycol	~	X	forms a very viscous gel
acetonitrile	X	✓	-5 mg product <b>1</b> + 100 µL → not soluble; dissolved in 1 mL - 30 mg mixture + 200 µL → side products completely dissolved

Table 12: RTD statistic in the SpinPro R10 for distilled water with various flow rates and rotation speeds at 25 °C.

$t_{\text{theoretical}}$ [min] <sup>a</sup>	flow rate [mL/min]	rotation speed [rpm]	$\bar{t}$ [min] <sup>b</sup>	Deviation in residence time [%]
<b>1.08</b>	19	1000	0.91	15 %
		3000	0.71	34 %
		4000	0.59	46 %
		5000	0.57	47 %
		6000	0.66	39 %
<b>2.16</b>	9.5	1000	1.56	28 %
		3000	1.61	25 %
		4000	1.30	39 %
		5000	1.56	27 %
		6000	1.42	34 %
<b>3.23</b>	6.3	1000	2.55	21 %
		3000	2.43	25 %
		4000	2.45	24 %
		5000	2.31	28 %
		6000	2.32	28 %
<b>4.30</b>	4.8	1000	3.45	20 %
		3000	3.28	25 %
<b>5.39</b>	3.8	1000	4.30	20 %
500 µM of rose bengal. <sup>a</sup> theoretical residence time. <sup>b</sup> mean residence time.				



Table 13: RTD statistic in the SpinPro R10 for 2 wt% HPMC E5 at various flow rates and rotation speeds.

$t^{\text{theoretical}}$ [min] <sup>a</sup>	flow rate [mL/min]	temperature [°C]	rotation speed [rpm]	$\bar{t}$ [min] <sup>b</sup>	Deviation in residence time [%]
<b>1.08</b>	19	25 °C	1000	0.62	42 %
			2000	0.51	47 %
			4000	0.49	55 %
		50 °C	1000	0.53	51 %
			2000	0.51	47 %
			4000	0.49	55 %
<b>2.16</b>	9.5	25 °C	1000	1.42	34 %
			2000	1.39	36 %
			4000	1.30	40 %
		50 °C	1000	1.43	34 %
			2000	1.36	37 %
			4000	1.36	37 %
<b>3.23</b>	6.3	25 °C	1000	2.30	29 %
			2000	2.17	33 %
			4000	2.06	36 %
		50 °C	1000	2.33	28 %
			2000	2.22	31 %
			4000	2.14	34 %
<b>4.30</b>	4.8	25 °C	1000	3.18	26 %
		50 °C	1000	3.17	26 %
<b>5.39</b>	3.8	25 °C	1000	4.03	25 %
		50 °C	1000	4.06	25 %

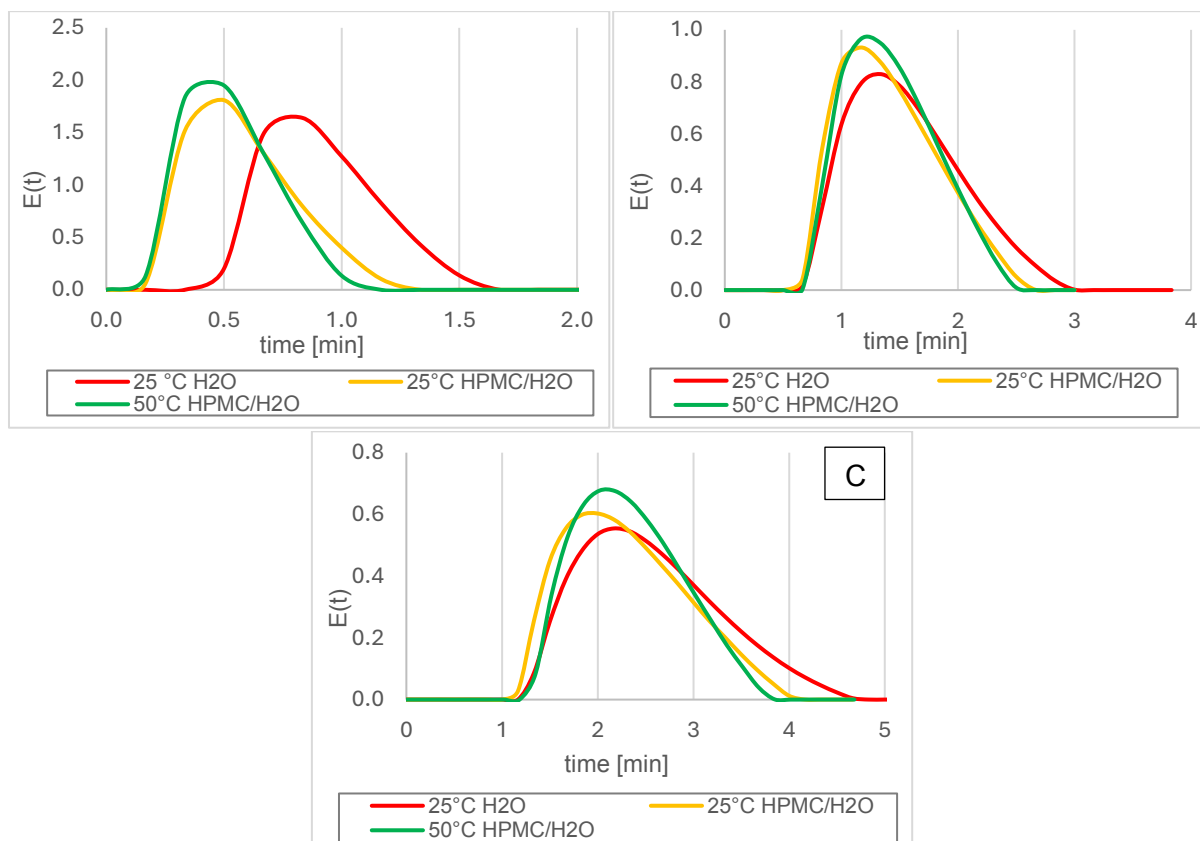
500  $\mu\text{M}$  of rose bengal. <sup>a</sup> theoretical residence time. <sup>b</sup> mean residence time.

Figure 15: RTD studies for different media in the SpinPro R10 at 1001 rpm. A – 19 mL/min; B – 9.5 mL/min; C – 6.3 mL/min.

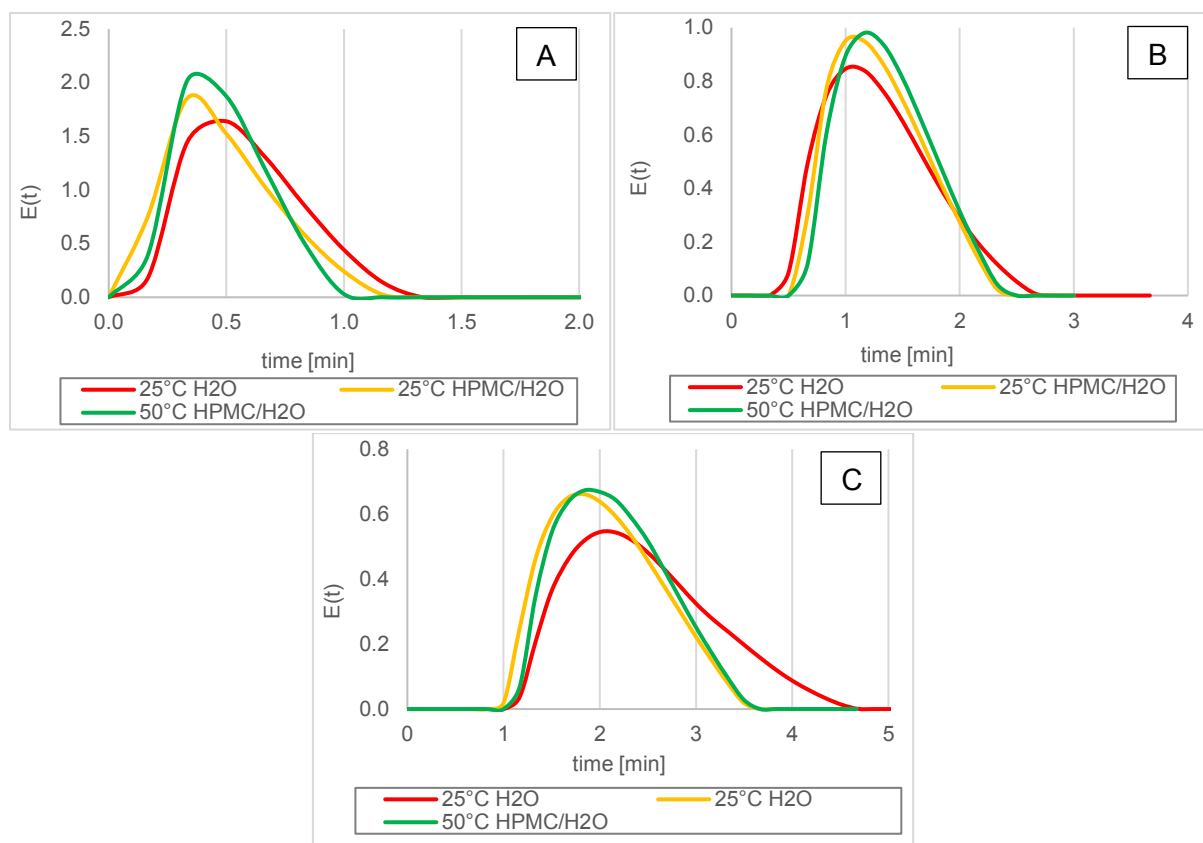


Figure 16: RTD studies for different media in the SpinPro R10 at 4000 rpm.  
A – 19 mL/min; B – 9.5 mL/min; C – 6.3 mL/min.

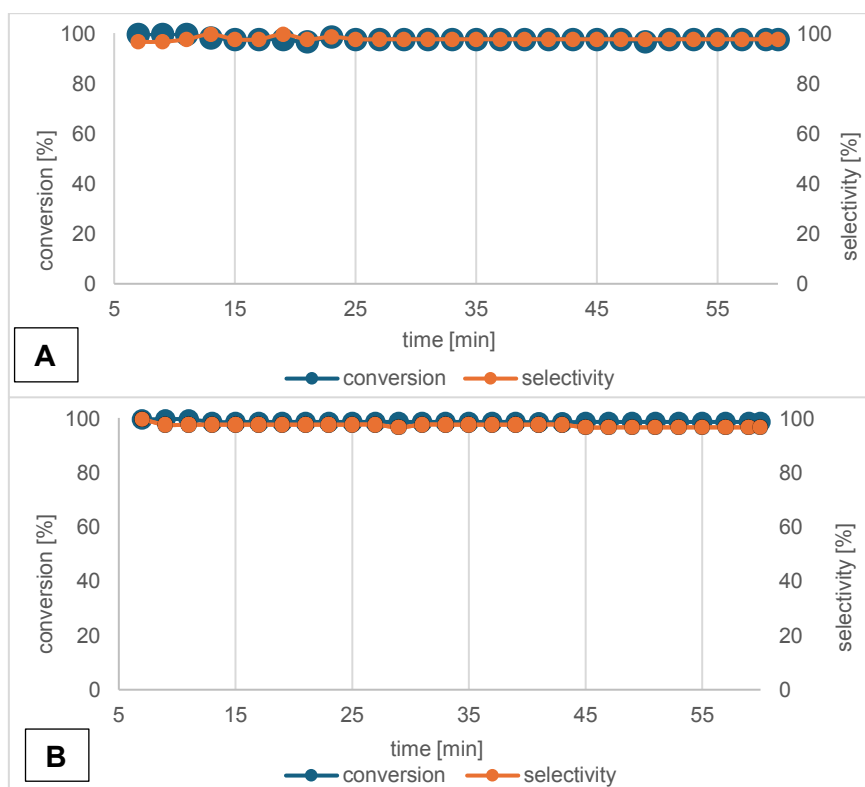


Figure 17: Stability tests for the synthesis of product 5 in the SpinPro R10. Conditions: 2000 rpm, 1 mL/min, A- 40 °C; B- 50 °C, 4-hydroxyphenyl acetic acid (1.1 M, 1.1 eq) and 2,6-lutidine (1.5 M, 1.5 eq) in 2 wt% HPMC/H<sub>2</sub>O (clear solution); 3,5-dimethylaniline (1.0 M, 1.0 eq) in 2 wt% HPMC/H<sub>2</sub>O (suspension); COMU (1.05 M, 1.05 eq) in 2 wt% HPMC/H<sub>2</sub>O (suspension). Samples were collected every 2 min.

Table 14: Values used for the assessment of green metrics for the synthesis of product 5 in flow with COMU.

role	chemical	equiv.	n [mmol]	m [g]	V [mL]	Mw [g/mol]	$\rho$ [g/cm <sup>3</sup> ]
REACTION							
substrate	1	1.0	9	13.69		152.15	
substrate	2	1.0	9	10.91	11.22	121.18	0.972
substrate	3	1.0	9	9.65	10.44	107.15	0.925
substrate	4	1.05	9.45	40.47		428.24	
solvent	EtOAc			643.68	720	88.11	0.894
PRODUCT							
product	5		9	22.96		255.13	

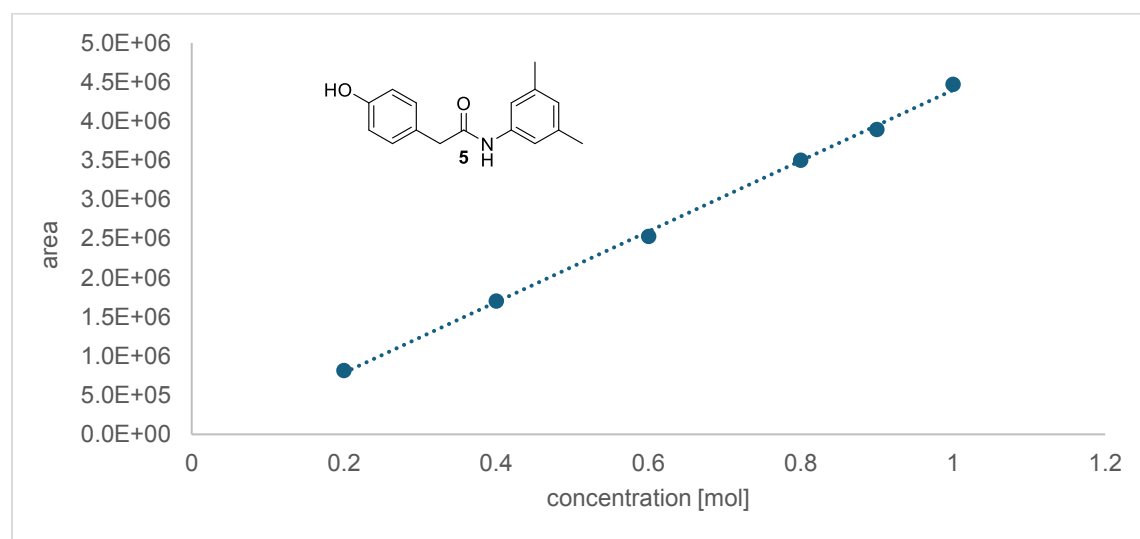


Figure 18: Calibration of product 5 measured with HPLC-UV/VIS at 215 nm.  $y = 4\,512\,382 - 115\,732x$ ;  $R^2 = 0.999$ . Dilution of the product was 1:1000 in analytical grade DMF, injection volume = 0.5  $\mu$ L.



Figure 19:  $^1\text{H}$ -NMR of the pure product, isolated from a flow run.  $^1\text{H}$  NMR (300 MHz,  $\text{DMSO-d}_6$ )  $\delta$ : 9.90 (s, 1H), 9.26 (s, 1H), 7.21 (d,  $J = 1.6$  Hz, 2H), 7.16 – 7.07 (m, 2H), 6.75 – 6.63 (m, 3H), 3.46 (s, 2H), 2.21 (s, 6H). Insignificant residues of EtOAc at 1.3 ppm, 1.9 ppm and 4.0 ppm. Solvent  $\text{DMSO-d}_6$  shows two peaks, one at 2.5 ppm and one at 3.3 ppm. Verified with literature.<sup>53</sup>

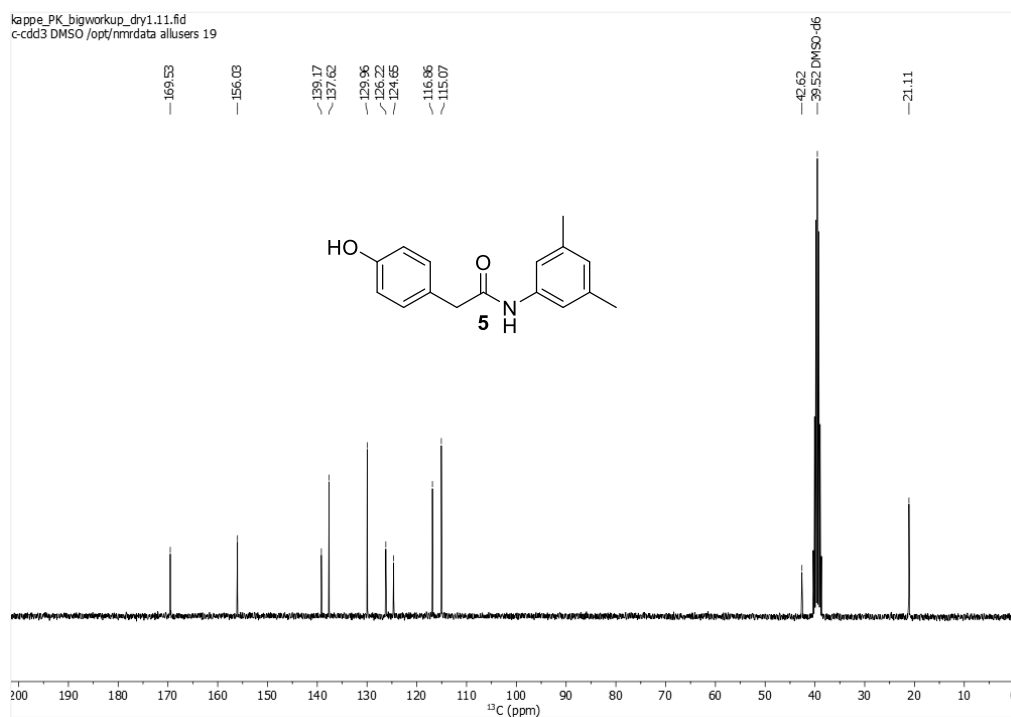


Figure 20:  $^{13}\text{C}$ -NMR of the pure product, isolated from a flow run.  $^{13}\text{C}$  NMR (75 MHz,  $\text{DMSO}$ )  $\delta$ : 169.53, 156.03, 139.17, 137.62, 129.96, 126.22, 124.65, 116.86, 115.07, 42.62, 21.11. No residues of EtOAc visible. Verified with literature.<sup>53</sup>